ACIBADEM MEHMET ALI AYDINLAR UNIVERSITY
GRADUATE SCHOOL OF HEALTH SCIENCES

# ANALYSIS OF GENETIC BIOMARKERS IN GLIOMA DIAGNOSIS AND PROGNOSIS: FOCUS ON *ECE1* rs3026809 VARIANT

GİZEL GERDAN

M.Sc. THESIS

DEPARTMENT OF GENOME STUDIES

SUPERVISOR
Assoc. Prof. Cemaliye AKYERLİ BOYLU

ISTANBUL-2026

ACIBADEM MEHMET ALI AYDINLAR UNIVERSITY
GRADUATE SCHOOL OF HEALTH SCIENCES

# ANALYSIS OF GENETIC BIOMARKERS IN GLIOMA DIAGNOSIS AND PROGNOSIS: FOCUS ON *ECE1* rs3026809 VARIANT

GİZEL GERDAN

M.Sc. THESIS

DEPARTMENT OF GENOME STUDIES

SUPERVISOR
Assoc. Prof. Cemaliye AKYERLİ BOYLU

ISTANBUL-2026

## DECLARATION

I declare that this thesis work is my own work, I had no unethical behavior at any stages from the planning to the writing of the thesis, I obtained all the information in this thesis in accordance with academic and ethical rules, I cited all the information and comments that were not obtained with this thesis work, and I provided resources in the list of references. I also declare that there was no violation of any patents and copyrights during the study and writing of this thesis.

06/05/2026
Gizel GERDAN

## PREFACE AND ACKNOWLEDGEMENT

First of all, I would like to express my endless gratitude to my dear mother, and my father who have supported me unwaveringly throughout my life and have always stood by me with their love.

During this thesis process, I would like to extend my sincere thanks to my advisor, Assoc. Prof. Cemaliye Akyerli Boylu. I am grateful not only for your academic guidance but also for your patience and understanding.

I would like to express my deepest thanks to all the academicians of the Department of Genome Studies, from whom I received knowledge and support on many subjects throughout the process, especially to Assoc. Prof. Kaya Bilgüvar. I would also like to sincerely thank Prof. Koray Özduman, who guided me with the provision of patient samples and insightful ideas; Prof. Ayça Erşen Danyeli, who did not withhold her valuable support in the field of pathology; Prof. Emel Timuçin for her invaluable contributions to my research journey and for the privilege of learning from her extensive knowledge; and Dr. Şirin Yüksel Kılıçturgay and Dr. Hilal Keskin Karakoyun, who added great value to this study through their efforts and contributions.

I would like to express my sincere thanks to Merve Nur Köroğlu Karakaya, Eylül Aydın, Aybike Bulut, and Alper Bülbül whose ideas I have always valued and who provided not only mentorship but also friendship during my thesis process. Also, thanks to my dear friends who stood by me throughout this journey: Jülide Ceren Yılmaz, and Leyla Ümit Laçin. All my friends who listened to my never-ending troubles in office A Block 511—your support was truly invaluable to me. I would also like to thank all my friends whose names I could not list here individually but who hold a special place in my heart. This work is dedicated to the memory of my grandfather, Bahri Gerdan. His inspiration guided my path, and his struggle with Klatskin tumor remains the driving force behind my research.

# TABLE OF CONTENTS

# ABBREVIATIONS AND SYMBOLS

| | |
|---|---|
| **AGT** | Angiotensinogen |
| **APC** | Adenomatosis Polyposis Coli Tumor Suppressor |
| **AS-PCR** | Allele-specific PCR |
| **ATRX** | ATP-Dependent Helicase |
| **BRAF** | B-Raf Proto-Oncogene |
| **BRCA1/2** | Breast and Ovarian Cancer Susceptibility Protein 1/2 |
| **CALCA** | Calcitonin Related Polypeptide Alpha |
| **CIC** | Capicua transcriptional repressor |
| **CGGA** | Chinese Glioma Genome Atlas |
| **CDKN2A/B** | Cyclin-Dependent Kinase Inhibitor 2A/B |
| **circRNAs** | Circular RNAs |
| **ClinVar** | Clinical Variants |
| **CNS** | Central Nervous System |
| **COSMIC** | Catalogue of Somatic Mutations in Cancer |
| **dNTPs** | Deoxynucleotide Triphosphates |
| **ddNTPs** | Dideoxynucleotriphosphates |
| **DMSO** | Dimethyl Sulfoxide |
| **ECE1** | Endothelin-converting enzyme-1 |
| **EGFR** | Epidermal Growth Factor Receptor |
| **EDN/ET** | Endothelin |
| **ETBR** | Endothelin B Receptor |
| **EtBr** | Ethidium Bromide |
| **FAP** | Familial Adenomatous Polyposis |
| **FUBP1** | Far Upstream Binding Protein |
| **GBM** | Glioblastoma |
| **GTEx** | Genotype-Tissue Expression |
| **HCSs** | Hereditary Cancer Syndromes |
| **HTB-138** | Hs683 cells human glioma cell line |
| **IDH** | Isocitrate Dehydrogenase |
| **KEL** | Kell Metallo-Endopeptidase |
| **Ki-67** | Antigen Kiel 67 |
| **LENG9** | Leukocyte Receptor Cluster Member 9 |
| **LGG** | Low-grade Gliomas |

| | |
|---|---|
| **LOEUF** | Loss-of-Function Observed/Expected Upper Fraction |
| **MGMT** | O-6-Methylguanine-DNA Methyltransferase |
| **MLH1** | MutL Homolog 1 |
| **MSH2/6** | MutS Homolog 2/6 |
| **mtDNA** | Mitochondrial DNA |
| **MYB/MYBL1** | Myeloblastosis / MYB Proto-Oncogene, Transcription Factor |
| **NES** | Normalized Effect Size |
| **OPCs** | Oligodendroglial Precursor Cells |
| **OR** | Odds Ratio |
| **PCR** | Polymerase Chain Reaction |
| **PMS2** | PMS1 Protein Homolog 2 |
| **RB1** | RB Transcriptional Corepressor 1 |
| **RFLP** | Restriction Fragment Length Polymorphism |
| **SLC9A1** | Solute Carrier Family 9 Member A1 |
| **SNP** | Single Nucleotide Polymorphism |
| **STRING** | Search Tool for the Retrieval of Interacting Genes/Proteins |
| **TERT** | Telomerase Reverse Transcriptase |
| **TCGA** | The Cancer Genome Atlas |
| **TF** | Transcription Factor |
| **TOP2A** | DNA Topoisomerase II Alpha |
| **TP53** | Tumor Protein P53 |
| **VUS** | Variants of Uncertain Significance |
| **WHO** | World Health Organization |

# LIST OF FIGURES

# LIST OF TABLES

# ABSTRACT

## Analysis of Genetic Biomarkers In Glioma Diagnosis and Prognosis: Focus On *ECE1* rs3026809 Variant

Gliomas are the most common primary brain tumors in adults and exhibit high molecular heterogeneity. Although conventional markers like 1p/19q co-deletion and *IDH* mutations are widely used in diagnosis, they may not provide a complete explanation of tumor behavior. To address this gap, the contribution of regulatory variants in gliomas was investigated. First, targeted sequencing data were analyzed using Ensembl VEP to examine regulatory alterations in 1p/19q-codeleted oligodendrogliomas, with a focus on regulatory variants across all genes on 1p and 19q. Selected variants were validated by Sanger sequencing and screened in glioma samples using AS-PCR and RFLP. The functional relevance was evaluated by in silico tools. The potential regulatory variant *ECE1*-rs3026809 (G>A) was observed in oligodendrogliomas (n=7/15) and GBM (n=9/9), but not in control (n=1). Statistical analysis was conducted to assess the association between rs3026809 and clinical data. The presence of the variant was significantly associated with tumor grade (p=0.0082), but not with Ki67 index (p= 0.173). Furthermore, pairwise analysis showed significant associations of Oligo3 (p= 0.005) and all oligodendroglioma grades (p= 0.009) with GBM. Additionally, logistic regression revealed strong associations with Ki67 index and tumor grade (accuracy = 90.5%), while differential expression analysis showed *ECE1* is upregulated in GBMs compared to LGGs. Notably, the genomic region harboring the variant is highly conserved across species, supporting its potential functional relevance. These findings suggest that rs3026809 may act as a regulatory modulator driving malignant progression, highlighting the importance of non-coding variants in gliomas and their potential for molecular stratification.



**Keywords**: Glioma, *ECE1* rs3026809, Regulatory biomarkers, Tumor aggressiveness, AS-PCR

# ÖZET


**Gliom Tanı ve Prognozunda Genetik Biyobelirteçlerin Analizi: *ECE1* rs3026809 Varyantına Odaklanma**

Gliomlar, yetişkinlerde en sık görülen primer beyin tümörleridir ve yüksek derecede moleküler heterojenlik gösterirler. Tanıda yaygın olarak kullanılan 1p/19q kodelesyonu ve *IDH* mutasyonları gibi klasik belirteçler, tümör davranışını tam olarak açıklamakta yetersiz kalabilir. Bu eksikliği gidermek amacıyla, gliomlarda düzenleyici varyantların katkısı araştırılmıştır. Çalışmanın ilk aşamasında, hedeflenmiş dizileme verileri Ensembl VEP ile analiz edilmiş ve 1p/19q kodelesyonu bulunan oligodendrogliomalarda, 1p ve 19q üzerindeki genlerde yer alan düzenleyici varyantlara odaklanılmıştır. Seçilen varyantlar Sanger dizileme ile doğrulanmış ve gliom örneklerinde AS-PZR ile RFLP yöntemleri kullanılarak taranmıştır. Fonksiyonel etkiler ise biyoinformatik tabanlı araçlarla değerlendirilmiştir. *ECE1* rs3026809 (G>A) düzenleyici varyantı, oligodendrogliomalarda (n=7/15) ve GBM'de (n=9/9) gözlenirken, kontrol grubunda saptanmamıştır (n=1). İstatistiksel analizler, bu varyantın tümör derecesi ile anlamlı şekilde ilişkili olduğunu göstermiştir (p=0.0082); ancak Ki-67 indeksi ile anlamlı bir ilişki bulunmamıştır (p=0.173). Ayrıca, ikili karşılaştırmalar Oligo3 (p=0.005) ve tüm oligodendroglioma derecelerinin (p=0.009) GBM ile anlamlı ilişkisini ortaya koymuştur. Ek olarak, lojistik regresyon analizi %90,5 doğrulukla Ki-67 indeksi ve tümör derecesi ile güçlü bir ilişki göstermiş; farklı gen ifade analizi ise, *ECE1*'in GBM'lerde DDG'lere kıyasla arttığını ortaya koymuştur. Varyantın bulunduğu genomik bölgenin türler arasında korunmuş olması, potansiyel fonksiyonel önemini desteklemektedir. Bu bulgular, rs3026809 varyantının kötü huylu tümör progresyonunu etkileyen düzenleyici bir modülatör olabileceğini ve gliomlarda kodlamayan varyantların moleküler sınıflandırma açısından önemini ortaya koymaktadır.



**Anahtar Sözcükler:** Gliom, ECE1 rs3026809, Düzenleyici biyobelirteçler, Tümör agresifliği, AS-PZR

# 1 INTRODUCTION AND AIM

Glial tumors (gliomas) are a heterogeneous group of neoplasms both histologically and molecularly, and they originate from neuroglial progenitor cells (1). They constitute the most frequent primary brain tumor in adults, account for approximately 30% of all central nervous system neoplasms (2) and represent about 80% of all malignant primary CNS tumors, making them the dominant malignant tumor group in the CNS (3). Gliomas have the typical features of cancer, such as long-term proliferative signaling, evasion of growth suppressors, apoptotic resistance, angiogenesis, invasion, and immune modulation. Treatment results are still inadequate despite major advancements in technology and medicine, mainly due to an incomplete understanding of glial tumor biology.

Gliomas are classified based on the specific type of glial cell involved; astrocytomas, oligodendrogliomas, and glioblastomas (4). Oligodendrogliomas are distinguished from glioblastomas by their lower aggressiveness and more favorable prognosis. Well-characterized markers such as 1p/19q co-deletion, *IDH*1/2 mutations, *ATRX* loss, *TP53* mutations, *EGFR* gene amplification, and *TERT* promoter alterations guide both classification and therapeutic strategies. While those molecular markers are well-known, they do not fully explain the heterogeneity or differences in tumor progression and treatment response. Therefore, the discovery of other biomarkers is essential to understand the biology of different tumor types and improve the risk stratification (4, 5).

On the other hand, regulatory region variants are gaining increasing attention in glioma biology due to their critical role in controlling gene expression; by influencing signaling pathways, extracellular matrix interactions, and the tumor microenvironment. These variants can drive inter-individual variability and contribute to tumor progression and aggressiveness (6).

To address these concepts, this research focuses on the analysis of regulatory alterations in 1p/19q-codeleted oligodendrogliomas, particularly within the chromosomal regions 1p and 19q. So far, two gene mutations (*CIC* on 19q and *FUBP1*

on 1p) have been identified in oligodendrogliomas; however, other alterations remain largely unknown (4). Our study involves a comprehensive evaluation of variants located in regulatory regions of all genes on these chromosome arms, followed by the investigation of functionally relevant variants for the diagnosis, prognosis, and treatment of glial tumors. Finally, the present work targets the resulting variants that may contribute to tumor aggressiveness.

The objectives of the study are as follows:

1. To investigate targeted sequencing data derived from oligodendroglioma samples, with a particular focus on regulatory regions of all genes (-650 bp to +250 bp allowing the target area to encompass regulatory elements as promoters and TF binding sites) on chromosomes 1p and 19q via Ensembl VEP
2. To identify key genetic variants within the analyzed region and evaluate their potential relevance to glioma biology and molecular heterogeneity.
3. To validate selected variants using Sanger sequencing to ensure accuracy.
4. To confirm and extend the analysis of defined variants across glial tumor types (including glioblastomas) by allele-specific PCR, and/or restriction fragment length polymorphism analysis.
5. To statistically analyze the identified variants and clinical data to assess their potential associations with tumor characteristics and clinical outcomes.
6. To evaluate the contribution of identified variants to tumor aggressiveness by comparing low-grade gliomas with glioblastomas and assessing their association with tumor progression.
7. To perform *in silico* analyses, including assessment of gene expression differences between glioblastoma and low-grade glioma, and protein–protein interaction network analysis in order to identify functionally related candidate genes and pathways.

In this study, mainly regulatory regions of genes within 1p and 19q were investigated rather than the extensively studied coding regions. To the best of our

knowledge, this is the first study—particularly in our country—to comprehensively evaluate regulatory genetic variations of these regions in glial tumors.

In this context, our study is expected to yield significant findings that may contribute to the prognosis of glial tumors. The identification of clinically relevant genomic alterations may ultimately facilitate their integration into clinical practice and improve patient stratification and management.

# 2 BACKGROUND

## 2.1 Cancer

Cancer, a collection of diseases marked by uncontrolled cell growth, stands as a primary cause of illness and death globally. It poses a substantial health challenge worldwide, with significant changes in epidemiology and etiology (7). Lung, breast, and colorectal cancers account for the majority of cancer cases worldwide according to Globcan (8). Specifically, in the United States, over 2 million new cancer cases and 600,000 deaths are presumed in 2024. In Türkiye, lung cancer is frequently observed, with an estimated 42 thousand cases according to Globcan. Advances in diagnosis, screening, and public health have reduced the incidence of certain cancers, such as gastric cancer rates in high-risk areas like Japan and South Korea (9). Even though cancer rates are rising among younger populations for other types, improvements vary across cancer categories. These rising trends are attributed to environmental factors, including lifestyle changes and genetic predispositions.

The majority of solid organ malignancies arise sporadically (about 80%), with multiple interacting factors contributing to increased susceptibility to one or more particular cancer types (10). None of these factors alone is sufficient or necessary to cause malignant transformation (11). Approximately 5-10% of cancers are associated with hereditary cancer syndromes (HCSs). These disorders, which are usually inherited in an autosomal dominant pattern, are caused by genetic alterations that increase vulnerability to cancer. Familial cancers account for 10-15% of cancers and refer to the occurrence of specific cancer within a family, which may result from genetic factors, shared environmental influences, or common lifestyle habits (12).

In the case of genetic risk factors, the pathogenesis of cancer is further complicated by mutations in oncogenes and tumor suppressor genes. For example, mutations in the *BRCA1 (*Breast and Ovarian Cancer Susceptibility Protein 1) and *BRCA2 (*Breast and Ovarian Cancer Susceptibility Protein 2) genes are closely linked to breast and ovarian cancers (13). Likewise, mutations in the *MLH1(*MutL Homolog 1)*, MSH2(*MutL Homolog 2)*, MSH6 (*MutL Homolog 6), and *PMS2 (*PMS1 Protein

Homolog 2) genes- which play essential roles in DNA mismatch repair-are connected to Lynch syndrome-significantly increasing the risk of colorectal and endometrial cancers (14). Additionally, mutations in the *TP53 (*Tumor Protein P53) gene lead to Li-Fraumeni syndrome, a disorder that predisposes individuals to an array of cancers, including sarcomas, brain tumors, and breast cancer (15). Other significant examples include mutations in the *APC (*Adenomatosis Polyposis Coli Tumor Suppressor) gene, which causes familial adenomatous polyposis (FAP) and drastically increase the likelihood of developing colorectal cancer, as well as mutations in the *RB1 (*RB Transcriptional Corepressor 1) gene, which are associated with retinoblastoma (16).

The common environmental risk factors for cancer include smoking, diet and nutrition, alcohol consumption, physical inactivity and obesity. Environmental and occupational factors can include: exposure to carcinogens and radiation or air pollution. Besides, prolonged exposure to ultraviolet radiation from the sun significantly raises the likelihood of developing skin cancers, such as melanoma (17). Infectious agents such as human papillomavirus and *Helicobacter pylori* also have an important role in cancer development (18).

Cancer is named after the tissue in which it first originates and is generally classified into six types. These are classified as carcinomas, sarcomas, leukemias, lymphomas, myelomas, and mixed type, which includes gliomas (Figure 1) (19).

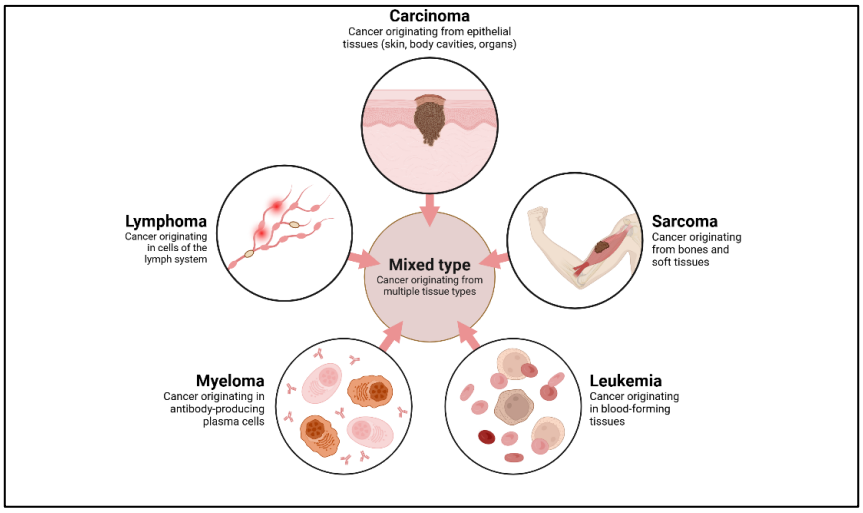


Figure 1. Histological classification of cancers

Diagrammatic representations of the main types of cancer by their tissue origin. Carcinoma, sarcoma, leukemia, myeloma, and lymphoma are the categories of malignancies. Mixed type cancers are developed from a combination of different tissue types (Created in BioRender.com)

### 2.1.1 Hallmarks of cancer

The Hallmarks of Cancer, initially proposed by Hanahan and Weinberg in 2000 and updated in 2011, 2022, and 2026, offer a conceptual model to understand the complex biological traits that allow cancer cells to survive, grow uncontrollably, and spread. The original framework outlined six critical capabilities that cancer cells acquire: sustained proliferative signaling, evasion of growth suppressors, activating invasion and metastasis, enabling replicative immortality, resistance to cell death, and the ability to induce angiogenesis. In 2022, Hanahan expanded the model further, introducing new hallmarks such as phenotypic plasticity and disrupted differentiation, non-mutational epigenetic reprogramming and the role of senescent cells in the tumor microenvironment as critical factors that help cancer cells acquire and sustain these hallmark traits. In 2026, in addition to acquired functional capabilities, new dimensions are added, focusing on hallmark-conveying cells populating cancer microenvironments and systemic interactions (20).

## 2.2 Human Nervous System

The brain consists of three main regions: the cerebrum, cerebellum, and brainstem. The cerebellum plays a crucial role in controlling motor functions and overall coordination of movements. Likewise, the cerebrum manages motor and sensory information and plays a key role in intelligence and memory functions (21). The brainstem regulates essential bodily functions, including motor and sensory control, cardiac and respiratory activity, and reflex actions (22).

### 2.2.1 Central nervous system tumors

Brain and other central nervous system (CNS) tumors contribute significantly to both mortality and morbidity across all age groups (23). With the help of the World Health Organization (WHO) 2021 classification scheme for CNS tumors, it has become easier to understand the categorization of 120 different types of brain tumors (24).

Gliomas and non-gliomas are two simple classifications of CNS tumors (1). Gliomas will be discussed further in detail; however, non-glioma tumors include meningiomas and pituitary adenomas. Other examples comprise primitive neuroectodermal tumors (medulloblastomas), primary CNS lymphomas, and infrequently occurring CNS germ cell tumors.

Advanced techniques like next-generation sequencing, RNA expression and DNA methylation profiling have enabled the reconceptualization of new super-categories and stratification of existing ones (25-27).

The American Cancer Society's projections for brain and spinal cord tumors in the United States for the year 2025 encompass cases among both adults and children (28). It is anticipated that approximately 25.000 malignant tumors affecting the brain or spinal cord will be diagnosed. Although precise statistics for adults and children remain unclear, this rate is estimated to be around 20% in pediatric oncology cases, which is distinct from adult-type cases in terms of disease progression (29).

## 2.3 Glial Tumors

Glial tumors, also referred to as primary gliomas, are among the most common primary brain tumors that arise from glial cells (30). They account for approximately 30% of all central nervous system neoplasms (2) and represent about 80% of all malignant primary CNS tumors (3). These tumors can be sorted into several categories, based on the specific type of glial cell involved like; astrocytomas, oligodendrogliomas, and ependymomas (Table 1) (24). Glioblastoma (GBM) accounts for approximately 50% of all gliomas and is most commonly observed in adults (31). GBM is the most prevalent malignant brain tumor, while meningiomas are the most common benign brain tumors (32).

Table 1. Overview of the WHO classification of glioma, glioneuronal and neuronal tumors

| **Family/Category** | **Types** |
|---|---|
| Gliomas, glioneuronal tumors and neuronal tumors | |
| Adult-type diffuse gliomas | • Astrocytoma, IDH-mutant,<br>• Oligodendroglioma, IDH-mutant and 1p/19q-codeleted<br>• Glioblastoma, IDH- wildtype |
| Pediatric-type low/high-grade diffuse gliomas | • Diffuse midline glioma, H3 K27-altered<br>• Diffuse hemispheric glioma, H3 G34-mutant<br>• Diffuse pediatric-type high grade glioma, H3 wildtype/IDH-wildtype<br>• Infant-type hemispheric glioma<br>• Others |
| Circumscribed astrocytic gliomas | • High-grade diffuse gliomas with pilocytic features<br>• Pilocytic astrocytoma<br>• Astroblastoma, MN1-altered<br>• Others |
| Glioneuronal, neuronal and ependymal tumors | • Diffuse glioneuronal tumor with oligodendroglioma-like features and nuclear clusters (DGONC)<br>• Diffuse leptomeningeal glioneuronal tumor<br>• Gangliоglioma<br>• Others |

The classification is according to the revised WHO guidelines of 2021; tumors are classified based on their histological or molecular characteristics. Adapted from (33).

Low-grade tumors, such as grade I and II gliomas, are typically characterized by slower growth rates, reduced metastatic potential, and a more favorable prognosis compared to high-grade tumors, which include grade III and IV gliomas, such as GBMs (24, 34, 35). Patients with low-grade oligodendrogliomas have a median survival of up to 11.6 years, whereas those with high-grade tumors, such as glioblastomas, exhibit a median survival of approximately 15 months (36).

Oligodendrogliomas, a distinct type of glioma, represent approximately 5–10% of all gliomas based on recent studies (37). They originate from oligodendrocytes, the myelinating cells of the brain. These tumors fall under the category of diffuse gliomas and are primarily classified based on their molecular characteristics, particularly the presence of Isocitrate Dehydrogenase (*IDH*) mutations and the co-deletion of chromosomal arms 1p and 19q (38-41). They generally have a more favorable prognosis compared to other gliomas, particularly when they harbor these molecular alterations, which are associated with better treatment responses and longer survival (42, 43).

### 2.3.1 Epidemiology of glial tumors

According to 2024 data, the age-adjusted incidence rate of brain and other CNS tumors worldwide has been reported as 3.5 per 100,000 individuals (44). This rate is 3.9 in males and 3.1 in females. It is estimated that approximately 321,731 individuals globally are diagnosed with primary malignant brain tumors (45).

For instance, GBM, the most common malignant brain tumor, accounts for 47.7% of all primary malignant brain tumors (46). The incidence rate of GBM is 3.21 per 100,000 individuals, and the median age at diagnosis is 64 years (47). It is frequently observed in males compared to females. The one-year survival rate is approximately 40%, while the two-year survival rate is around 17% (48).

The exact incidence rate of low-grade gliomas (LGG) remains uncertain, as the implementation of the WHO CNS classification among tumor registries is still in its early stages (49). However, it is known that, LGGs are more frequently observed in younger individuals, typically between the ages of 20 and 40. The peak incidence varies by tumor type, with oligodendrogliomas most diagnosed between ages 40 and 45, whereas astrocytomas tend to peak between ages 30 and 40. Additionally, similar to GBM, low-grade gliomas exhibit a slightly higher prevalence in males (50).

### 2.3.2 Molecular alterations in glial tumors

Significant genetic alterations that influence targeted therapies and prognostic evaluations have been identified in various CNS tumors. These include Epidermal Growth Factor Receptor (*EGFR*) amplification in the classical subtype of glioma (51), *BRAF (*B-Raf Proto-Oncogene) V600E mutations in juvenile low-grade gliomas, and *IDH1/2* mutations in gliomas, all of which are detected through molecular profiling (52).

Besides these, mutations in ATP-Dependent Helicase (*ATRX)* are frequently observed in astrocytomas with *IDH* mutations and in diffuse hemispheric gliomas (53). GBMs often exhibit homozygous deletions of Cyclin-Dependent Kinase Inhibitor 2A/B (*CDKN2A/B)* (54), which contribute to their aggressive behavior. Alterations like O-6-Methylguanine-DNA Methyltransferase *(MGMT)* promoter methylation are associated with enhanced chemotherapy sensitivity, especially in glioblastomas (55). Other notable genetic changes include my-elob-lastosis/ MYB Proto-Oncogene, Transcription Factor (*MYB/MYBL1)* alterations, Telomerase Reverse Transcriptase (*TERT)* promoter mutations, and *TP53* mutations, which play a role in characterizing distinct glioma subtypes and predicting their clinical outcomes. Capicua transcriptional repressor (*CIC)* and far upstream binding protein (*FUBP1)* are key tumor suppressor genes frequently mutated in oligodendrogliomas (56). According to COSMIC, *CIC* was altered in 51%, while *FUBP1* mutations were observed in 21% of cases. More common *CIC* (19q) mutations affect transcriptional repression, while *FUBP1* (1p) mutations influence *MYC*-related transcriptional regulation; both contributing to glioma development and classification (57). Overall molecular alterations in brain tumors are summarized in Figure 2.

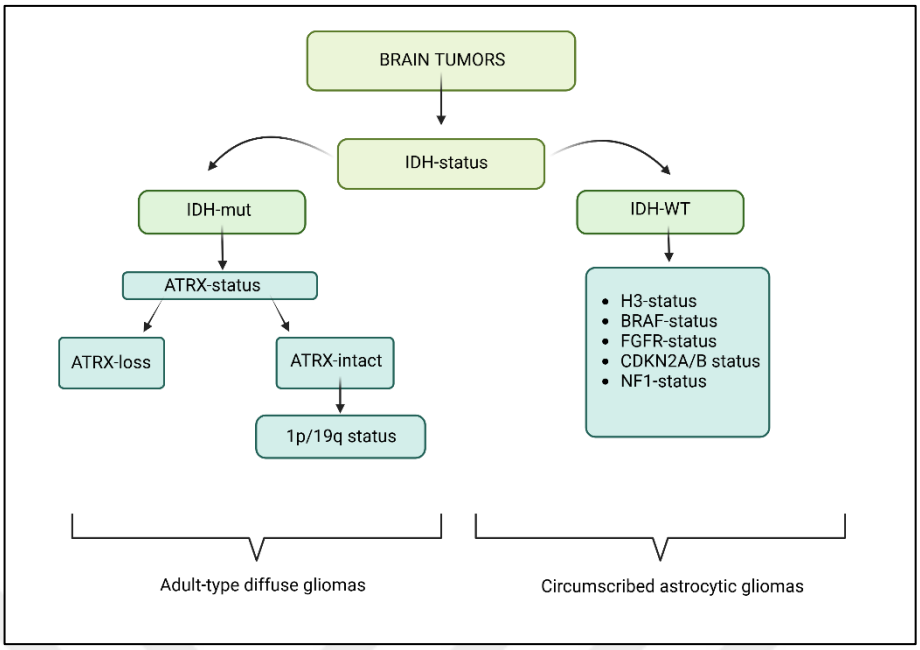


Figure 2. Overview of molecular alterations in brain tumors

Flowchart of the diagnostic path according to the key genomic alterations. Adapted from (58) (Created in Biorender.com).

### 2.3.3 Other molecular alterations in glial tumors

In addition to these common alterations, glial tumors exhibit a broad spectrum of genetic and epigenetic changes that contribute to glial tumor development, progression, and therapeutic resistance. According to recent research, endothelin-converting enzyme-1 (*ECE1)* may promote invasiveness in cancers like prostate, GBM and oligodendrogliomas (59). *ECE1* specifically facilitates the transformation of inactive big endothelin-1 (*ET1*) into its active form (60). Active *ET1* has been implicated in various adult cardiovascular conditions, Hirschsprung disease and autonomic dysfunction (61). Moreover, elevated *ECE1* levels have also been detected in several malignancies, where high expression is associated with poor prognosis and contributes to the development of androgen independence in prostate cancer (62).

In a recent study, the presence of *ECE-1c* (an isoform of *ECE1*) was linked to enhanced invasive behavior and overall malignancy in GBM. *ECE1c* mutant was designed by switching ubiquitination lysine proximal to the phospho-serines Lys-6-to-

Arg. This ECE1cK6R mutant was stably expressed in GBM cell lines- U87MG, T98G, and U251 and cells' behavior was compared to WT *ECE1c*-expressing clone cells (63). Since there was no ubiquitination, degradation does not occur, leading to increased *ECE1* expression in cells.

Another study investigating the function and expression of circular RNAs (circRNAs) in GBM, reveals that CircNDC80 (cNDC80)- a circular RNA that is synthesized from *NDC80* gene by circularization of exons 14 to 17- is upregulated and associated with *ECE1* expression. Basically, cNDC80 functions as a sponge for miR-139-5p. circRNA bounds to the miRNA and blocks the function, therefore acts as a "sponge". When cNDC80 blocks miR-139-5p, it cannot bind to *ECE1*. Hence, when *ECE1* is overexpressed, it promotes GBM development. These were also supported through bioinformatic tools such as miRanda, TargetScan, PicTar, miRWalk and ENCORI. It has been observed that there is a strong correlation between miR-139-5p and *ECE1*. In addition, Chinese Glioma Genome Atlas (CGGA) was scanned through and different findings were found, which are: miR-139-5p levels decrease when the grade of cancer increases, indicating that the tumor represses the miRNA. When the grade of cancer increases, the *ECE1* expression also increases and if the *ECE1* expression is low, the prognosis is much more positive. These correlations suggest that there is a tumor suppressor/oncogene relationship between miR-139-5p and *ECE1* (64).

Regarding oligodendroglioma, the function of the endothelin B receptor (ETBR) has been investigated with respect to its impact on patient survival and tumor proliferation. ETBR expression construct was transfected into Hs683 cells-human glioma cell line (HTB-138). In this case, the intention was to specifically knockdown ETBR gene expression. Therefore, it is possible that ETBR activation plays a crucial role in tumor progression, since it stimulates the proliferation of oligodendroglioma cells (65).

Furthermore, DNA Topoisomerase II Alpha (*TOP2A)*, a key decatenating enzyme that modifies DNA topology by binding to two double-stranded DNA molecules, has been associated with transcriptional changes in GBM (66). Through NGS sequencing a novel variant E948Q has been linked to increased DNA binding and relaxation activity, as well as decreased patient survival (67).

### 2.3.4 Mitochondrial DNA variations and glial tumors

While mutations in mitochondrial genes are frequently observed in cancer cells, they typically do not disable mitochondrial energy metabolism. Instead, they modify the bioenergetic and biosynthetic state of the mitochondria (68). Malignant tumors, including gliomas, prefer abnormal energy production through aerobic glycolysis and exhibit intrinsic resistance to apoptosis (69). Mitochondrial DNA (mtDNA) methylation contributes to copy number changes and tumorigenesis in GBM (70). While mtDNA methylation is reduced and copy number is eleveated during the initial stages of tumor progression, methylation levels subsequently increase once tumorigenesis is triggered by a critical mtDNA copy number threshold. This late-stage event in tumorigenesis limits mtDNA replication and keeps mtDNA copy numbers lower in GBM cell lines compared to non-tumorigenic cell lines (71). In Grade II and III glioma cells, elevated oxidative stress is associated with the impaired mitochondrial function and a higher number of mutations in the coding regions of mtDNA (72).

### 2.3.5 Importance of intronic variants in glial tumors

Mutations occurring within introns have the potential to disrupt regulatory elements or splice sites, which can result in abnormal splicing events (73). These events may produce oncogenic isoforms or interfere with the functions of tumor suppressor genes. Intronic variants are gaining significant attention for their involvement in the molecular mechanisms of glial tumors. Despite not directly encoding proteins, these regions play a crucial role in regulating gene expression and RNA splicing, two processes that maintain cellular stability (74).

Regarding oligodendrogliomas, mutations within intronic sequences can interfere with normal RNA splicing by either modifying spliceosome recognition sites or creating cryptic splice sites (74). These molecular disturbances can drive tumor formation by impacting critical regulatory pathways, including those responsible for the cell cycle control, DNA repair, and programmed cell death (apoptosis)(75).

## 2.4 Sanger Sequencing

Sanger sequencing is one of the first-generation DNA sequencing techniques to determine the nucleotide sequence of a DNA fragment by using DNA polymerase to extend a primer. It is the confirmatory step of any mutation screening method and still has a vital role in clinical genomics (76). The Sanger dideoxy chain termination method relies on usage of both 3'-labeled fluorescent dideoxynucleotriphosphates (ddNTPs) and normal deoxynucleotides (dNTPs) during DNA extension reactions. The random incorporation of a dideoxynucleotide terminates DNA synthesis, producing fluorescently labeled DNA fragments of varying lengths that can then be separated via capillary electrophoresis and analyzed by software. However, despite improvements in sequencing chemistry and heterozygote-detection software, direct automated sequencing of PCR products does not guarantee complete mutation detection, especially when using tumor samples (77).

## 2.5 Allele-Specific PCR

Allele-specific PCR (AS-PCR) also known as "amplification refractory mutation," is a highly sensitive, accurate technique and is carried out to identify single nucleotide alterations in DNA sequences with the help of primers selective for an allele. The method is based on the primers that are complementary to the target sequence at the 3' end, thereby enabling selective amplification for either the wild-type (WT) or mutant allele, allowing accurate detection of genetic variation (78). The low cost and quick agarose gel detection of the amplified products are the benefits of the basic AS-PCR (79). Additionally, this technique is primarily applied in cancer research, since mutation detection is hugely relevant to cancer diagnosis and management.

## 2.6 Restriction Fragment Length Polymorphism

Restriction endonucleases recognize specific short DNA sequences and cleave double-strand DNA at defined sites either within or near these sequences. These recognition sequences are typically 4 to 6 nucleotides long and are often characterized by palindromic structures (80). Some restriction enzymes cleave at the axis of symmetry yielding “blunt” ends, whereas others make staggered cleavages yielding “sticky” ends. Incubating the enzyme with the DNA under the proper reaction conditions results in restriction enzyme cleavage. By using these restriction enzymes to examine variations within DNA sequences, Restriction Fragment Length Polymorphism (RFLP) is an appropriate molecular technique used in cancer research. This method utilizes restriction enzymes resulting in fragments of different lengths that reflect genetic differences among individuals. The generated fragments are subsequently separated through gel electrophoresis, enabling the visualization of these genetic variations (81).

## 2.7 Resources For Bioinformatics In Genomic Research

Bioinformatics tools are important for the functional interpretation of genomic variants. These resources enable the evaluation of both coding and non-coding variants, along with their potential regulatory effects and tissue-specific expression patterns. Furthermore, when combined with robust statistical analyses and the integration of protein–protein interaction networks, the biological significance of the identified variants becomes more evident.

### 2.7.1 COSMIC, CLINVAR and TCGA databases

The COSMIC (Catalogue of Somatic Mutations in Cancer) and Clinical Variants (ClinVar) databases offer crucial insights into the genetic profile of glial tumors. COSMIC catalogs somatic mutations in tumors, aiding in the identification of cancer-driving mutations and their roles in tumorigenesis. In contrast, ClinVar mostly focuses on germline variants, helping to identify pathogenic mutations linked to hereditary cancer syndromes. Recent findings from COSMIC and ClinVar underscore key

mutations in genes such as *IDH1, TP53*, and *EGFR*, which are frequently mutated in glial tumors. Together, these databases are essential tools for identifying biomarkers, advancing precision medicine, supporting ongoing research into the molecular mechanisms underlying glial tumors, and they are suitable for guiding preliminary investigations. On the other hand, The Cancer Genome Atlas (TCGA) is a publicly available database used for identifying genomic alterations in various cancers, aiming to build a comprehensive atlas of cancer genomic landscapes (82).

### 2.7.2 Tools and databases for variant analysis

Comprehensive annotation of coding and non-coding variants is supported by Ensembl Variant Effect Predictor (VEP), which offers insights into the possible biological effects of these variations (83). Additionally, to check the phylogenetic context of the variants through the UCSC Genome Browser, regulatory elements can be investigated using JASPAR CORE motifs, to identify transcription factor binding sites (84) while RegulomeDB combines various epigenomic and eQTL data to assess the regulatory potential of non-coding loci (85). Genotype-Tissue Expression (GTEx) provides tissue-specific expression patterns (86). STRING provides a system-level view of gene relationships by depicting protein interactions and functional networks (87). For statistical evaluation of genomic and clinical data, platforms such as JAMOVI allow accessible analysis and interpretation of research findings.

# 3 MATERIALS AND METHODS

## 3.1 Materials

### 3.1.1 Patient samples

Clinical samples were obtained from Acıbadem Mehmet Ali Aydınlar University, Department of Neurosurgery- Prof. M. Necmettin Pamir and Prof. Koray Özduman. Our study was approved by the Acıbadem Mehmet Ali Aydınlar University Ethics Committee with the approval number ATADEK-2024-10/395 (Supplementary 8.2). All participants signed informed consent and research volunteer forms (Supplementary 8.1). Adult cohort biological samples (blood and tumor tissues) of the Acıbadem University Brain Tumor Research Group were used for further genomic analysis.

### 3.1.2 Standard solutions and buffer solutions

| | |
|---|---|
| 50X TAE Buffer (Tris- Acetic Acid-EDTA): | 242 g tris base in double-distilled $H_2O$<br>57.1 ml glacial acetic acid<br>100 ml 0.5 M EDTA solution (pH 8.0) |
| 10X TAE Buffer: | 48.5 g tris base<br>11.4 ml glacial acetic acid<br>20 ml 0.5M EDTA (pH 8.0)<br>The volume was adjusted to 1000 ml by double-distilled $H_2O$ |
| 1X TAE Buffer: | 100 ml 10X TAE Buffer<br>900 ml double-distilled ($ddH_2O$) $H_2O$ |
| 10X TBE Buffer (Tris - Boric Acid - EDTA): | 108 g tris base<br>55 g boric acid<br>40 ml 0.5 M EDTA solution (pH 8.0)<br>The volume was adjusted to 1000 ml by double-distilled $H_2O$ |

| | |
|---|---|
| 1X TBE Buffer: | 100 ml 10X TBE Buffer<br>900 ml double-distilled $H_2O$ |
| 30% Acrylamide-Bisacrylamide Stock Solution (19:1): | 142.5 g Acrylamide<br>7.5 g Bisacrylamide<br>The volume was adjusted to 500 ml by $ddH_2O$ |
| 20% Acrylamide-Bisacrylamide Working Solution: | 6.67 ml 30% Acrylamide-Bisacrylamide Stock<br>2 ml 5X TBE<br>1.23 ml $ddH_2O$<br>100µl 10% APS<br>5µl TEMED |
| 7% Acrylamide Gel | 11.76 ml 30% Acrylamide-Bisacrylamide Stock<br>800 µl APS<br>0.5 ml 50X TAE<br>11.94 ml $ddH_2O$ |
| 0.6% Agarose with TEMED | 0.3 g Agarose<br>25 ml 1X TAE<br>40 µl TEMED |
| 5X Gel loading buffer | 0.25% bromophenol blue<br>0.25% xylene cyanol<br>50% glycerol<br>1mM EDTA |

### 3.1.3 Sterile distilled $H_2O$ for PCR

The water to be used for polymerase chain reaction (PCR) was aliquoted in 1.5 ml Eppendorf tubes as 1000 µl portions from a sterile distilled water bottle. It was incubated at 85°C for 15 minutes. After cooling, it was stored at +4°C, ready for use.

### 3.1.4 Devices

| DEVICES | SUPPLIER |
|---|---|
| Shaker | Solaris Shaker- Thermo Scientific |
| Fume hood | Tezsan, Türkiye |
| Electrophoresis power supply | Power-Pac-Basic – Bio-Rad, USA |
| Electrophoresis tank | Sub-Cell GT- Bio-Rad, USA |
| Precision balance | Adventurer Pro – Ohaus, USA |
| Heating block | Witeg, Germany |
| Gel imaging system | ChemiDoc MP – Bio-Rad, USA |
| Micropipette set | FINNPIPETTE F2- (P10, P20, P200, P1000) – Thermo Scientific |
| pH meter | Inolab – WTW, Germany |
| Centrifuge | Biofuge pico – Heraeus, Germany |
| Thermal cycler | T100 Thermal Cycler– Bio-Rad, USA |
| Vortex | Velp Scientifica, Italy |
| Nanodrop | NanoDrop One$^C$- Thermo Scientific |

| DEVICES | SUPPLIER |
|---|---|
| Shaking Water Bath | WF-SBC30, Weightlab Instruments |
| Vertical Electrophoresis | Bio-Rad Mini-PROTEAN Tetra System - Bio-Rad, USA |

### 3.1.5 Chemicals and kits

| CHEMICAL/KIT | SUPPLIER |
|---|---|
| **DNA Isolation** | |
| Ethanol | Merck, Germany |
| QIAamp DNA Mini Kit | Qiagen, USA |
| 1X Phosphate-buffered saline (PBS) | Thermo Scientific, USA |
| **PCR (Polymerase Chain Reaction)** | |
| Deoxynucleotide triphosphates (dNTPs) | Thermo Scientific, USA |
| Dimethyl sulfoxide (DMSO) | Sigma-Aldrich, USA |
| Taq DNA Polymerase | Fermentas, USA |
| Sterile distilled water | Eczacıbaşı-Baxter, Türkiye |
| DMSO | Sigma-Aldrich, USA |
| **Gel Electrophoresis** | |
| Agarose | Applichem, Germany |
| Boric acid | Sigma-Aldrich, USA |
| EDTA | Applichem, Germany |

| CHEMICAL/KIT | SUPPLIER |
|---|---|
| Ethidium bromide (EtBr) | Sigma-Aldrich, USA |
| Generuler 100 bp DNA Ladder | Thermo Scientific, USA |
| Generuler 50 bp DNA Ladder | Thermo Scientific, USA |
| Tris-Base | Sigma-Aldrich, USA |
| Glacial acetic acid | MERCK, Germany |
| APS | Bio-Rad, USA |
| TEMED | Thermo Scientific, USA |
| Acrylamide | Bio-Rad, USA |
| Bisacrylamide | A.B.T., Türkiye |
| Xylene cyanol | Sigma-Aldrich, USA |
| Glycerol | Sigma-Aldrich, USA |
| Bromophenol blue | MERCK, Germany |
| **Restriction Enzyme** | |
| *CviKI*-1 Restriction Enzyme | New England Biolabs, USA |
| 1X CutSmart Buffer | New England Biolabs, USA |
| **PCR Product Purification** | |
| ExoSAP-IT | Affymetrix, USA |

### 3.1.6 Glass and plastic materials

Glass bottles (250, 500, and 1000 ml) used in the preparation of solutions and buffer solutions were obtained from Isolab (Germany). Eppendorf tubes (200, 500, and

1500 µl), pipette tips (10, 20, 200, and 1000 µl), and plastic plates were supplied by Axygen (USA).

### 3.1.7 dNTP cocktail

The dNTP cocktail was prepared using individual nucleotide solutions, dATP, dCTP, dGTP, and dTTP to achieve a final concentration of 10 mM each. Each nucleotide was combined in equimolar concentrations with $ddH_2O$ according to the manufacturer's instructions, gently mixed thoroughly and centrifuged. The prepared dNTP mix was aliquoted in 50–100 µl portions and stored at −20 °C.

### 3.1.8 Oligonucleotides

Oligonucleotides were designed using Primer3web (v.4.1.0). Primers used in PCR, AS-PCR and Sanger sequencing (Table 2), were synthesized by Sentebiolab (Ankara, Türkiye).

Table 2. Sequence and properties of the primers

| Primer (F/R) | Sequence (5'—> 3') | %GC | Tm | Amplicon Size | Used For |
|---|---|---|---|---|---|
| ECE-1 F<br>ECE-1 R | **TGACAGAGGAGCAGAGGTGT**<br>**TTGGCCACACTGCAAAGAAG** | 55.0<br>50.0 | 58ºC | 368 bp | PCR |
| ECE-1_WT_F<br>ECE-1_MUT_F<br>ECE-1_AS_R | **TGCATGCATGGGGTGGCG**<br>**TGCATGCATGGGGTGGCA**<br>**GTTTAAAAGAAGCGGAGCAGGA** | 66.7<br>61.1<br>45.5 | 60ºC | 158 bp | AS-PCR |

The primer tubes were delivered in lyophilized (freeze-dried) form by the supplier. Each primer was centrifuged at 13,000 rpm for 1 minute, and the amount of PCR-grade sterile distilled $H_2O$ specified by the manufacturer was added to dissolve the primers to a 50 µM stock concentration. The primers were then aliquoted in 50 µl volumes and stored at -20°C. For use in experiments, the primers were diluted with sterile distilled $H_2O$ to a working concentration of 5 pmol/µl.

## 3.2 Methods

### 3.2.1 Patient samples

Table 3. Clinical and Molecular Profiles of Oligodendroglioma, GBM and Control Cases

| DNA ID | Grade | Age | Gender | Anatomic Location | 1p/19q status | mtDNA_Variation_Counts* | 8q24_CCDC26_rs55705857* | *IDH1** | *TERT** |
|---|---|---|---|---|---|---|---|---|---|
| 13-95 | Oligo2 | 46 | F | L-Frontal | co-deleted | ND | WT | R132H | C250T |
| 12-46 | Oligo2 | 31 | M | L-Frontal | co-deleted | 14 (6/14 same w/control) | A/G | R132H | C228T |
| 13-30 | Oligo2 | 40 | M | R-Lateral Sulcus | co-deleted | 14 (5/14 same w/control) | WT | R132H | C228T |
| 14-146 | Oligo2 | 28 | F | L-Frontal | co-deleted | ND | WT | R132H | C228T |
| 14-147 | Oligo2 | 44 | M | L-Frontal | co-deleted | ND | A/G | R132H | C228T |
| 14-177 | Oligo2 | 32 | M | L-Central | co-deleted | ND | WT | R132H | C250T |
| 13-1023 | Oligo3 | 37 | M | R-Frontal | co-deleted | ND | WT | R132H | C250T |
| 13-03 | Oligo2 | 40 | M | R-Frontal | co-deleted | 30 (11/30 same w/control) | WT | R132H | C228T |
| 13-865 | Oligo2 | 38 | M | R-Frontaperiatal | co-deleted | ND | WT | R132H | C250T |
| 12-18 | Oligo2 | 29 | M | L-Frontal | co-deleted | ND | WT | R132H | C250T |
| 12-65 | Oligo2 | 39 | M | L-Temporal | co-deleted | 16 (7/16 same w/control) | A/G | R132H | C228T |
| 14-34 | Oligo3 | 47 | M | R-Occipital | co-deleted | ND | A/G | R132H | C228T |
| 14-163 | Oligo3 | 35 | F | L- Posterior Temporal | co-deleted | ND | WT | R132H | C228T |
| 13-708 | Oligo3 | 28 | F | L- Posterior Frontal | co-deleted | 3 (1/3 same w/control) | A/G | R132H | C228T |
| 13-739 | Oligo3 | 31 | F | L-Frontal | co-deleted | ND | WT | R132H | C228T |
| 14-195 | Control | 27 | M | Temporal Tissue | not | ND | WT | WT | WT |
| 13-606 | GBM | 67 | M | R-Frontal | not | ND | WT | WT | C228T |
| 13-713 | GBM | 78 | F | Cerebellum | not | ND | WT | WT | C250T |
| 12-54 | GBM | 54 | M | L-Occipital | not | ND | WT | WT | C228T |
| 12-75 | GBM | 56 | F | R-Frontal | not | ND | WT | WT | C228T |
| 12-102 | GBM | 56 | M | R-Occipital | not | ND | WT | WT | C250T |
| 12-105 | GBM | 44 | M | R-Periatal | not | ND | WT | WT | C228T |
| 13-716 | GBM | 64 | F | L-Frontal | not | ND | WT | WT | C228T |
| 13-720 | GBM | 56 | M | R-Temporal | not | ND | WT | WT | C250T |
| 13-821 | GBM | 63 | F | L-Occipital | not | ND | WT | WT | C228T |

Summary of demographic information and genomic changes of oligodendroglioma (n=15), glioblastoma (GBM, n=9), and control (n=1) cases. Molecular data comprises co-deletion status of 1p/19q, mitochondrial (Mt) alterations, and variant status of IDH, TERT, and 8q24 CCDC26 variant and the 1p/19q status. Abbreviations: WT, wild type; L, left; R, right.
*data provided by Acıbadem University Brain Tumor Research Group

Clinical and molecular information was systematically accessed to make an integrated patient profile; including age, sex, tumor grade, and accurate anatomic localization of the tumor (Table 3). Tumor locations were identified (e.g. left frontal, right lateral sulcus, left central, posterior temporal) with further notes that displayed extension to the opposite lobes or radiological characteristics such as microvascular proliferation. Each case was characterized at the molecular level with the evaluation of 1p19q codeletion state, *IDH* mutation, *TERT* promoter changes, and the 8q24 (*CCDC26* rs55705857).

### 3.2.2 Genomic DNA isolation

Genomic DNA was extracted using the "QIAamp DNA Mini Kit" in accordance with the manufacturer's instructions from peripheral blood samples stored at -80°C, tumor samples stored in liquid nitrogen, and sections obtained from paraffin blocks stored at room temperature.

#### 3.2.2.1 DNA isolation from peripheral blood

Peripheral blood samples, which had been stored at -80°C, were first thawed at room temperature. From each sample, 200 µl was carefully transferred into clean Eppendorf tubes. Then, 200 µl of Lysis Buffer (AL) and 20 µl of Proteinase K were added. The mixtures were then vortexed thoroughly to combine the contents and incubated at 56°C for 10 minutes to facilitate lysis.

Following the incubation step, 200 µl absolute ethanol was added to each tube to assist in DNA precipitation. The samples were mixed again using a vortex and transferred into filter tubes. The filter tubes were centrifuged at 10,000 rpm for 1 minute to separate the lysate, and the collection tubes underneath the filters were discarded.

Next, the filters were placed into new clean tubes, and 500 µl Washing Solution I (AW1) was added. The samples were centrifuged at 10,000 rpm for 1 minute. This washing process was repeated using 500 µl of Washing Solution II (AW2) to ensure the DNA was free of contaminants.

To dry the filters, they were centrifuged at 13,000 rpm for 1 minute. Subsequently, the filters were transferred to clean eppendorf tubes, and 200 µl of Elution Buffer (AE) was added to elute the DNA. After allowing the samples to rest at room temperature for 1 minute, they were centrifuged at 10,000 rpm for 1 minute and the extracted DNA was collected. Elution with volumes of less than 200 µl increases the final DNA concentration in the eluate significantly but slightly reduces the overall DNA yield. Short-term storage was maintained at +2°C to +8°C, while -20°C was used for long-term storage.

The concentration and purity of the isolated DNA were assessed using spectrophotometric measurements at wavelengths of 260 nm and 280 nm with the NanoPhotometer Pearl device. In each case, 1µl DNA sample was applied to the device and samples with an A260/A280 ratio ranging from 1.8 to 2.0 were considered to be of high purity.

#### 3.2.2.2 DNA isolation from tumor samples stored in liquid nitrogen

Tissue samples stored in liquid nitrogen were transferred to a petri dish at room temperature. Small pieces of tissue, collectively weighing no more than 25 mg, were taken from all corners of the tissue and collected in an Eppendorf tube. After adding 500 µl of 1X PBS, the samples were mixed using a vortex and centrifuged at 5,000 rpm for 5 minutes. The PBS was removed from the tissue pellet and 200 µl of Tissue Lysis Buffer (ATL) and 20 µl of Proteinase K were added. The mixture was vortexed thoroughly and incubated overnight at 56°C.

For completely dissolved samples, 200 µl Lysis Buffer (AL) was added, and the samples were incubated at 70°C for 1 hour. For partially dissolved samples, an additional 20 µl Proteinase K was added, and the samples were incubated for an additional hour before proceeding to the 70°C incubation step. After incubation, 200 µl of absolute ethanol was added to the samples, and the same procedure was followed as for peripheral blood.

#### 3.2.2.3 DNA isolation from sections obtained from paraffin blocks

Before isolating DNA from paraffin blocks stored at room temperature, a deparaffinization process was carried out. Sections with a thickness of 50 microns were placed in an Eppendorf tube. 1000 µl of xylene was added, and the mixture was vortexed thoroughly. The samples were then incubated at 56°C for 10 minutes to facilitate deparaffinization. After incubation, the samples were centrifuged at 13,000 rpm for 1 minute, and the supernatant containing the xylene was discarded.

Next, 1000 µl of absolute ethanol was added to the precipitate. The samples were mixed thoroughly using a vortex and centrifuged again at 13,000 rpm for 1 minute.

This ethanol washing was repeated once more and twice with sterile distilled water to ensure thorough washing. After the final centrifugation step, the samples were left to dry with their caps open at 56°C for at least 10 minutes to allow any residual liquid to evaporate completely.

The deparaffinized samples were then processed for DNA isolation. To each tube, 200 µl Tissue Lysis Buffer (ATL) and 20 µl of Proteinase K were added. The samples were mixed thoroughly using a vortex and incubated overnight at 56°C. From this point on, the procedure followed was identical to that for isolating DNA from tumor tissues stored in liquid nitrogen.

### 3.2.3 Preliminary research conducted by Acıbadem University Brain Research Group: Targeted sequencing

Targeted sequencing was conducted using the HiSeq 2500 platform with a 2x100 bp read configuration. The resulting data was generated and subsequently provided by the client via ftp in fastq format. The sequencing reads originated from a total of 16 samples, consisting of one normal sample and 15 oligodendroglioma samples, all of which underwent targeted capture specifically for chromosome 1 and chromosome 19, with a particular focus on the 1p and 19q regions.

The average Illumina quality scores for all samples exceeded Q30 at 101 bp, indicating high sequencing accuracy across the study. Adapter sequences were removed from the samples, ensuring that over 99.5% of the reads were completely free of adapter contamination. Additionally, any 3' bases with a quality score below 15 were trimmed, though less than 1% of the total data required trimming due to low-quality scores. For alignment, the human reference genome hg19 was used, yielding an alignment rate of approximately 91.5%, with normal paired-read gap distributions ranging between 200 and 500 bp. After the removal of adapters and low-quality sequences, more than 99% of the original reads remained intact. This resulted in an average of approximately 20 million 2x101 bp reads available for whole genome alignment.

Notably, around 65% of identified mutations were found on the targeted chromosomes (Chr 1 & 19), despite these regions constituting only about 32% of the total captured sequence data. The overall alignment rate reached 92%, yet a significant portion of sequencing coverage was spent on non-target regions. This inefficiency suggests that optimizing the capture probe hybridization process could lead to substantial cost savings and improved genome coverage. By implementing even moderate improvements in probe hybridization, sequencing costs could be reduced while simultaneously enhancing single nucleotide polymorphism (SNP) detection rates.

### 3.2.4 Polymerase chain reaction

The regions covering the *ECE1* rs3026809 variant were amplified by PCR in a total volume of 50 µl, using 50–100 ng of genomic DNA. The final concentrations were set as 1X Taq Buffer, 1.5 mM $MgCl_2$, 200 µM dNTP, 5 pmol forward and reverse primers each (ECE-1 F and ECE-1 R)(Table 2), and 1U Taq DNA Polymerase and nuclease-free water to complete the final volume. PCR conditions were optimized as in Table 4. All PCR products were analyzed on 2% agarose gel.

The second-round PCR was carried out when the first-round amplicons were faint under the same conditions as the first-round PCR.

#### 3.2.4.1 PCR conditions

Table 4. PCR Conditions

| Step | Temperature | Duration | Cycles |
|---|---|---|---|
| Initial Denaturation | 96°C | 3 minutes | 1 |
| Denaturation | 94°C | 30 seconds | 35 |
| Annealing | 58°C | 30 seconds | |
| Extension | 72°C | 30 seconds | |
| Final Extension | 72°C | 5 minutes | 1 |
| Holding Temperature | 4°C | Infinite | |

Overview of the temperature, time and cycle parameters used in the standard PCR protocols.

### 3.2.5 Agarose gel electrophoresis

PCR products were analyzed through horizontal gel electrophoresis using 1X TAE/1X TBE as the running buffer. The gel was prepared by combining 2g of agarose and 100 ml 1X TAE/TBE in a bottle. The mixture was heated in a microwave until the agarose was completely dissolved, resulting in a uniform and homogenous solution. After allowing the gel solution to cool slightly, 0,9 µl ethidium bromide (EtBr) (final concentration of 30-50 ng/ml) was added under a fume hood to the gel, for DNA visualization under UV light.

The PCR amplicons were mixed with a loading dye, using a volume equivalent to 1/5 of the sample volume. The mixtures were then carefully loaded into the wells of the agarose gel. Electrophoresis was conducted at 80V for a duration of 45-50 minutes. To facilitate the determination of product sizes, a DNA marker, 100 bp ladder was loaded alongside the samples.

### 3.2.6 Sanger sequencing

Prior to Sanger sequencing, first or second-round PCRs were purified using the Applied Biosystems ExoSAP-IT™ PCR Product Cleanup Reagent, according to the

manufacturer's instructions. The Applied Biosystems ABI 3730xl DNA Analyzer and BigDye Terminator Chemistry was successfully used to analyze the target gene regions across all the samples. Sequence alignment with reference sequences revealed several variations, including SNPs and small insertions/deletions (indels). The sequencing analysis was performed in both directions using the amount of PCR recommended by the manufacturer's instructions- MSM/Macrogen Europe (İstanbul, Türkiye) as an outsourced service.

### 3.2.7 Allele-Specific PCR

AS-PCR was performed to genotype the rs3026809 (G/A) variant using the above-mentioned PCR amplicons (368 bp) as a template. For each sample, two separate PCR reactions were done to distinguish the wild-type (G ) and the mutant (A) alleles by using different primer sets; the first primer set (*ECE-1* WT-F/AS-R) and the second primer set (*ECE-1* MUT-F/AS-R). Each 50 µl reaction mixture consisted of 1X Taq Buffer, 1.5 mM $MgCl_2$, 200 µM dNTP, 5 pmol forward and reverse primers each (*ECE-1* WT-F, *ECE-1* MUT-F, and *ECE-1* AS-R; (Table 2), 1U Taq DNA Polymerase, 5µl of PCR products (368 bp PCR amplicon), and nuclease-free water to complete the final volume. During optimization, 5% (v/v) dimethyl sulfoxide (DMSO) was added to the master mix to enhance specificity; however, as it did not improve amplification performance, it was excluded in further experiments. PCR conditions were adjusted through gradient annealing temperature trials, and the final optimized parameters are presented in Table 5. The resulting PCR products (158 bp) were analyzed on 2.5% agarose gel electrophoresis. Visualized through Bio-Rad ChemiDoc Imaging System.

During optimization, *ECE1* AS-PCR forward primers (WT and MUT) were additionally paired with *ECE1* reverse primer (*ECE1* R), generating a 192 bp amplicon. Nevertheless, for definitive results, only the AS-PCR primer pairs were employed in subsequent experiments.

Table 5. AS-PCR Conditions

| Step | Temperature | Duration | Cycles |
|---|---|---|---|
| Initial Denaturation | 96°C | 3 minutes | 1 |
| Denaturation | 94°C | 30 seconds | 35 |
| Annealing | 60°C | 30 seconds | 30 |
| Extension | 72°C | 30 seconds | 35 |
| Final Extension | 72°C | 5 minutes | 1 |
| Holding Temperature | 4°C | Infinite | 1 |

Overview of the temperature, time and cycle parameters used in the AS-PCR protocols.

### 3.2.8 Restriction fragment length polymorphism

10 µl of PCR product was incubated with 1U of *CviKI*-1 in a total reaction volume of 20 µl, using the recommended buffer (1X CutSmart Buffer) provided by the manufacturer. Following an optimization of the digestion protocol, incubation was performed in a water bath at 37°C for 1 hour. In cases where incomplete cleavage was observed, the duration was extended to 2 hours to ensure full enzymatic activity. Since *CviKI*-1 does not have a recommended heat inactivation protocol, 5 µl Loading Buffer was added into each reaction. To visualize the digested fragments, reactions were loaded on first 4% and 3% agarose gels excluding EtBr and ran with 1X TAE for approximately 2 hours at 50V. Then, the gel was stained in 300µl distilled $H_2O$ containing 150-200ng EtBr and put on shaker for 20 minutes. After, the gel was destained for 5 minutes in distilled $H_2O$ on the same platform and visualized through Bio-Rad ChemiDoc Imaging System. As a second option, 7% Acrylamide + 0.6% Agarose Gel containing TEMED- was prepared and ran with 1X TAE for 2 hours at 50V. Finally, 20% Native PAGE Gel was preferred as third option and ran with 1X TBE buffer, at 70V for 2 hours, vertically. The staining and destaining methods were all the same for all gels as mentioned above.

### 3.2.9 Resources for bioinformatics in genomic research

Ensembl VEP was used to analyze annotated variants, considering all available annotation features, such as pathogenicity prediction scores, and allele frequencies. Moreover, phylogenetic context is checked by making a multiple alignment, choosing ‘’92 eutherian mammals EPO-Extended’’ and all possible species. Additionally, tissue-specific expression in the central nervous system were checked throughout GTEX. To check for somatic and germline reported variants of *ECE1* and specifically rs3026809, COSMIC (filtered as: CNS>Brain>Glioma>Not Specified) and ClinVar were used. The UCSC Genome Browser was utilized to access JASPAR CORE motifs, which provides predicted TF binding locations, represented by shaded boxes. According to UCSC JASPAR CORE 2024 database, the intensity of the shading correlates with the p-value of the profile's match to the binding site, with scores ranging from 0 to 1000—where 0 corresponds to a p-value of 1, and 1000 corresponds to a p-value $\leq 10^{-10}$. A lower (better) p-value results in a darker shade of the boxes (84). To evaluate potential transcription factor binding sites of the *ECE1* rs3026809, JASPAR is used. The regulatory potential of rs3026809 (G>A) was estimated using RegulomeDB scores by integrating chromatin accessibility.

### 3.2.10 RNAseq and DESeq2 analysis

Gene sets used for RNAseq and DESeq2, were retrieved from TCGA data (accessed January 3, 2026). The systematic process of identifying differentially expressed genes between LGG (TCGA-LGG) and GBM (TCGA-GBM) using The Cancer Genome Atlas (TCGA) (dbGaP Study Accession: phs000178) RNA sequencing data was performed.

Initially, data was retrieved for both tumor types, and filtered as:

- Experimental Strategy ‘’RNA-Seq’’
- Data Format ‘’tsv’’
- Access ‘’open’’
- Tissue Type ‘’tumor’’

- Tumor Descriptor ‘’primary’’

comprising 288 cases for GBM, and 516 cases for LGG.

Analysis was then rigorously performed using the ‘’differential expression analysis for RNA-seq data package (version 2) (DESeq2) R package’’, which is specifically designed for RNA-Seq count data, to compare gene expression profiles of LGG versus GBM. A crucial filtering step was followed, involving the elimination of duplicates and recurrence patients. Resulting final set of genes represents the potential molecular signature distinguishing these two distinct glioma types.

### 3.2.11 Protein–Protein Interaction (PPI) network analysis

Using STRING, functional associations between ECE1 and other candidate genes were investigated. Furthermore, a protein–protein interaction (PPI) network analysis was performed using GeneMANIA, Reactome, and KEGG pathway databases to identify genes functionally and biologically associated with ECE1. Intersection analysis was conducted by applying log2 fold-change and adjusted p-value (padj) filters. For each gene, the presence of variants was checked within our research group’s targeted sequencing dataset.

### 3.2.12 Statistical analysis

Statistical analyses were performed using the JAMOVI software package (version 2.6.26). To explore the relationship between the rs3026809 (G/A) variant and patients’ clinical data, descriptive statistics were first generated for all variables. A correlation matrix analysis was conducted to examine potential interactions among quantitative clinical parameters, including age, tumor grade, gender, Ki-67 index, and molecular markers such as *IDH* and *TERT*. Prior to the *t*-tests, assumptions of normality and homogeneity of variance were evaluated using the Shapiro–Wilk and Levene’s tests, respectively. $P$ values $<0.05$ were considered statistically significant. Haldane-Anscombe correction was applied to odds ratio (OR) by adding each and every cell of the 2 x 2 table by 0.5, which stabilizes the amount of variance and allows one to estimate the effect size correctly (88). This approach enhances the robustness and

interpretability of statistical estimates, particularly in the presence of rare variants and small sample sizes.

# 4 RESULTS

## 4.1 Patient Samples

Our patient cohort consists of 15 cases of oligodendroglioma (Oligo2 and Oligo3) and 9 cases of GBM. 1 normal temporal tissue was included as control in the analysis. Oligodendroglioma patients were significantly younger, with a mean age of 36.3 years, in contrast to GBM patients, who had a mean age of 59.8 years. Both groups showed a male predominance; oligodendrogliomas had 10 males (67%) and 5 females (33%), while GBMs had 5 males (56%) and 4 females (44%). Regarding anatomic location, oligodendrogliomas have a strong preference for the frontal lobe. 8 of the15 cases arise in the frontal lobe (6 on the left side and 2 on the right side). GBMs exhibited a broader anatomical distribution, with 2 cases in the right frontal and 2 left occipital regions, and individual cases in the cerebellum, right occipital, right parietal, left frontal, and right temporal areas. Proliferative activity, as assessed by Ki67 index, was higher in GBMs (mean 23.6%) compared to oligodendrogliomas (mean 5.4%). All samples were included in variant analysis.

## 4.2 Preliminary Targeted Sequencing: Variant Filtering and Key Variant Decision

Sequencing analysis revealed a diverse pool of variants in the 1p and 19q regions, with *TTC34* and *ZNF* genes emerging as the most frequently mutated gene groups in oligodendrogliomas. Over one hundred fifty thousand non-unique variants across the cohort were identified and the number of variants that differ from the control is summarized in Figures 3 and 4.

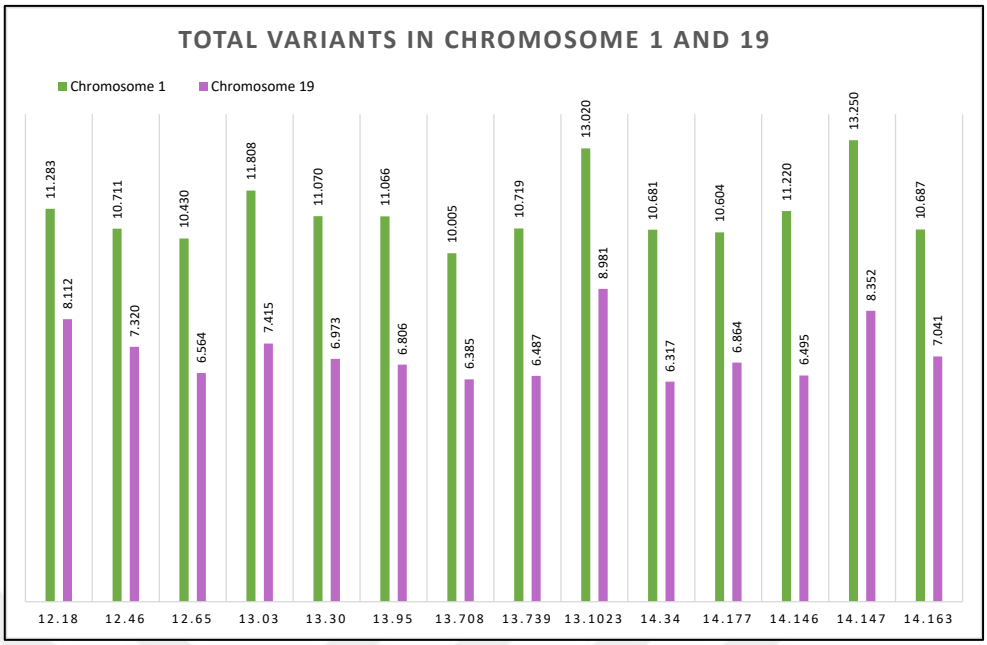


Figure 3. Total variants identified in chr 1 and chr 19

Comparison of the overall genomic variants detected per sample from targeted sequencing. Green bars indicate variants at Chromosome 1, and purple bars indicate variants at Chromosome 19. The x-axis shows DNA IDs, and above each bar, there is a numerical value that represents the number of a particular variant of that chromosome. Reported values reflect the overall number of variants, including non-unique ones.

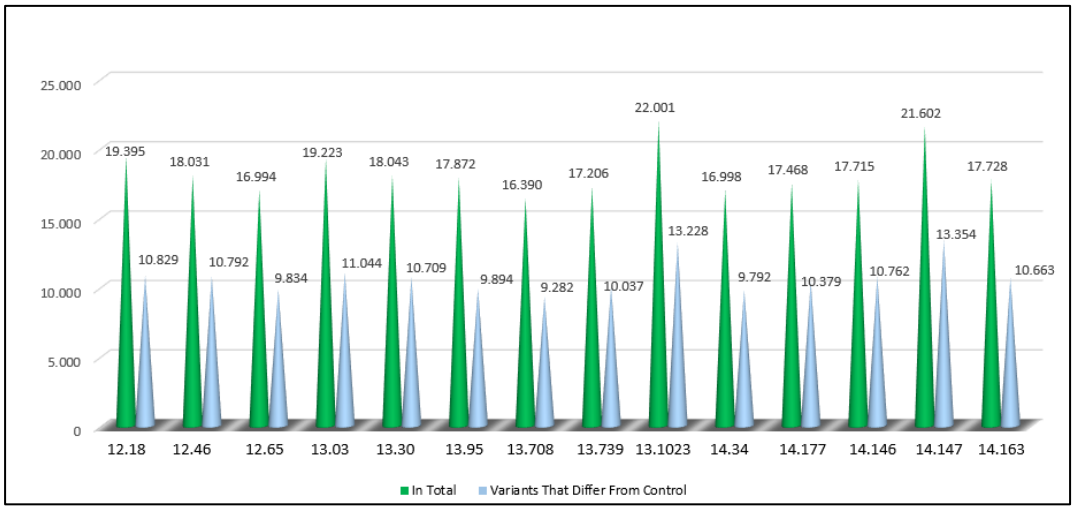


Figure 4. Total variant count and variants differing from control

Total detected variants in both chromosomes (Figure 3) for each patient sample are represented with green. Number of variants unique to each sample compared to the control is represented with blue. X-axis shows DNA IDs.

Variant analysis filtering was done as; >/= 15x coverage, and mutation score of >/= 12. At the end, the total number of high confidence mutations in Chromosome 1 and 19 as 914 and 393 were detected, respectively. Alignment rate was ~92% → ~19 million reads. So, aligned base was 3.838 Gb. While this data analysis was not a classic Tumor Mutational Burden, the large number of variants observed within regulatory regions of 1p and 19q suggests a regional mutational burden that could have functional implications in tumor progression.

Gene classification was done through variants with the highest and lowest recurrence across all patients. Throughout those variants, prevalent gene & gene families were observed, differing from the control: *ZNF* families, *TTC34*, *GP6* and *PSG3* genes being the most prevalent. On the other hand, *ECE1, JAK1*, and *SAMD11* genes (Figure 5) were rarely observed throughout the total variants. There were others but variants of *ECE1* drew attention with their biological properties.

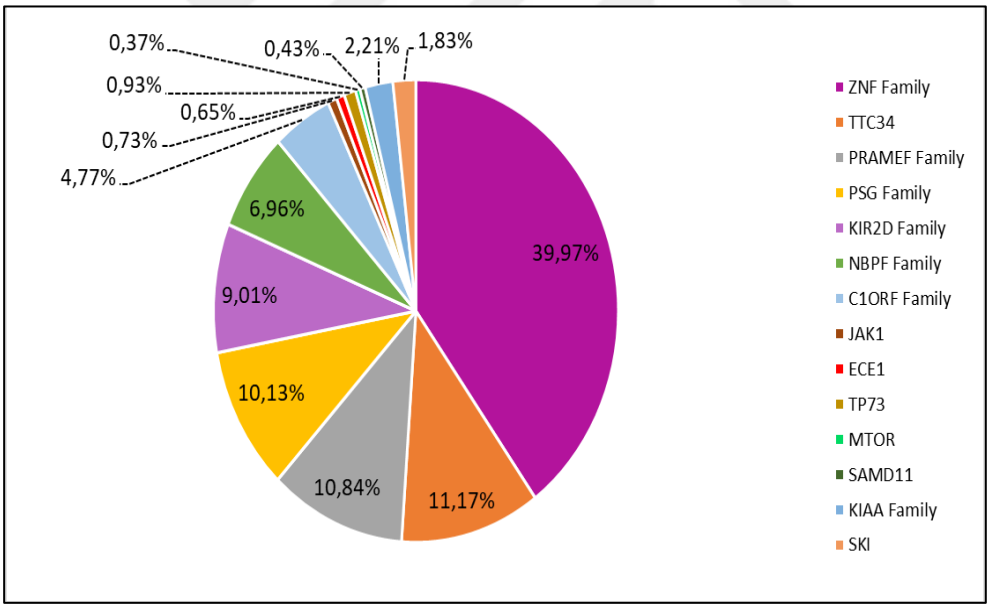


Figure 5. Distribution of patient-specific rare variants according to genes/gene families

The chart categorizes variants that are uncommon among patients. The *ZNF* family accounts for the largest proportion of these filtered variants (39.97%), reflecting a heterogenous collection of distinct variants distributed across multiple genes within the family. Certain genes such as *ECE1, JAK1* and *SAMD11* were the least common in this rare pool of variants. These identified variants differ from the control sample.

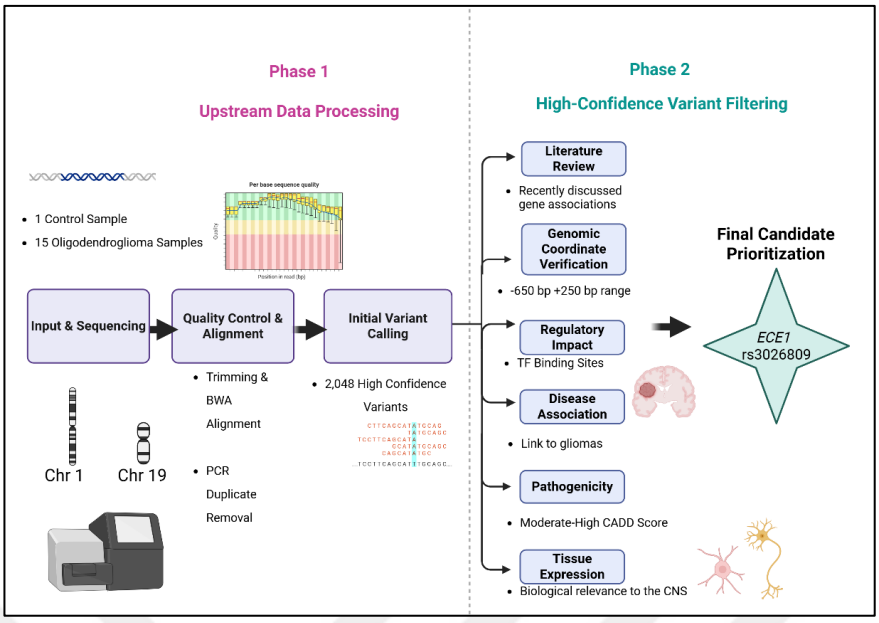


Figure 6. Workflow of key variant determination process

Schematic illustration of the two-phase pipeline that determined the candidate variant for this study.

In Figure 6- Phase 1 (Upstream Data Processing), genomic data obtained from 15 oligodendroglioma tumor samples and one control sample were subjected to targeted sequencing. The raw sequencing data was first evaluated through quality control procedures, including read trimming and alignment to the reference genome using BWA, followed by PCR duplicate removal to ensure data reliability. After that, an initial variant calling step was performed, resulting in the identification of 2,048 high-confidence variants located within the targeted chromosomal regions, especially on chromosome 1p and chromosome 19q.

In Phase 2 (High-Confidence Variant Filtering), variants were filtered and prioritized via criteria, including: literature review to identify previously reported gene associations, genomic coordinate verification within the regulatory region of interest (−650 bp to +250 bp), and assessment of regulatory impact like potential transcription factor (TF) binding sites. Ensembl VEP (Variant Effect Predictor) was used to analyze variants of 15 targeted-sequenced patient samples (except one control sample) with all of the existing annotation options: frequencies, predictors, and regulatory features, enabling the key variant decision. Still, variants were filtered critically for the 1p and 19q chromosomal regions, focusing on exons 1–2 and mainly first intronic regions, to

capture functionally relevant alterations. As variants were detected by default from regions beyond 1p and 19q, including non-targeted regions, a stringent filtering process was applied. Further filtering steps involved evaluating disease associations with gliomas, predicting pathogenicity scores (e.g., CADD), and assessing tissue-specific gene expression related to the CNS. Through this integrative prioritization strategy, the variant *ECE1* rs3026809 emerged as the relevant candidate for further functional investigation. Here, for instance, missense variants- at exon 1 of Leukocyte Receptor Cluster Member 9 *(LENG9)* and Killer Cell Immunoglobulin Like Receptor, Two Ig Domains and Long Cytoplasmic Tail 3 (*KIR2DL3)* genes were found as a result of the annotation, commonly observed in all patients. rs10406453 has a CADD score of 3.55 and rs62124153 has -0.033. Those two variants were not previously related to glial tumors and further investigation was not performed in our study.

### 4.3 *ECE1* rs3026809 Variant

*ECE1* rs3026809 was identified in 7 out of 15 oligodendroglioma and all in 9 GBM patients analyzed but were not detected in the control sample.

In Figure 7, the protein structure of *ECE1* is illustrated having cytoplasmic and catalytic domains, a transmembrane region, and a zinc-binding motif within the catalytic domain. This variant is located on chromosome 1p, at position 21,342,867, with a reference nucleotide C and an alteration to T, also represented as *ECE1* (NM_001113348.2): c.3+2509G>A. According to Ensembl VEP, its allele frequency is 0.3433, while gnomAD reports a frequency of 0.4093. *ECE1* has 19 exons and rs3026809 (G>A) is an intronic alteration located in intron 1. It is well known that G>A transitions are common in gliomas, particularly in GBMs. For instance, studies indicate that approximately 97% of mutations in hypermutated gliomas are C>T/G>A transitions (89). Highly conserved profile is found throughout primates, mammals (Figure 8), and rodents with a few exceptions.

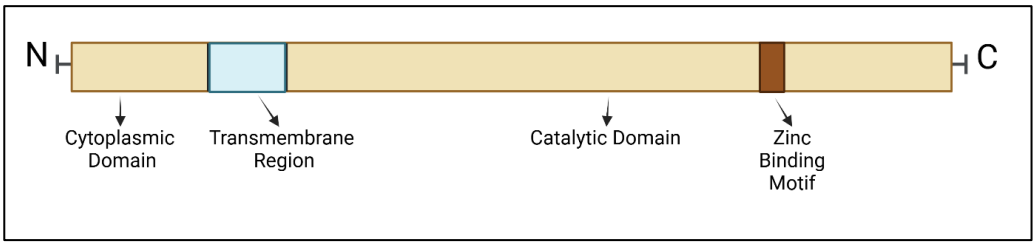


Figure 7. ECE1 and its functional regions

Structural organization and functional domains of the ECE1. The N- and C-termini represent the start and end of the polypeptide chain, respectively. Adapted from (59).

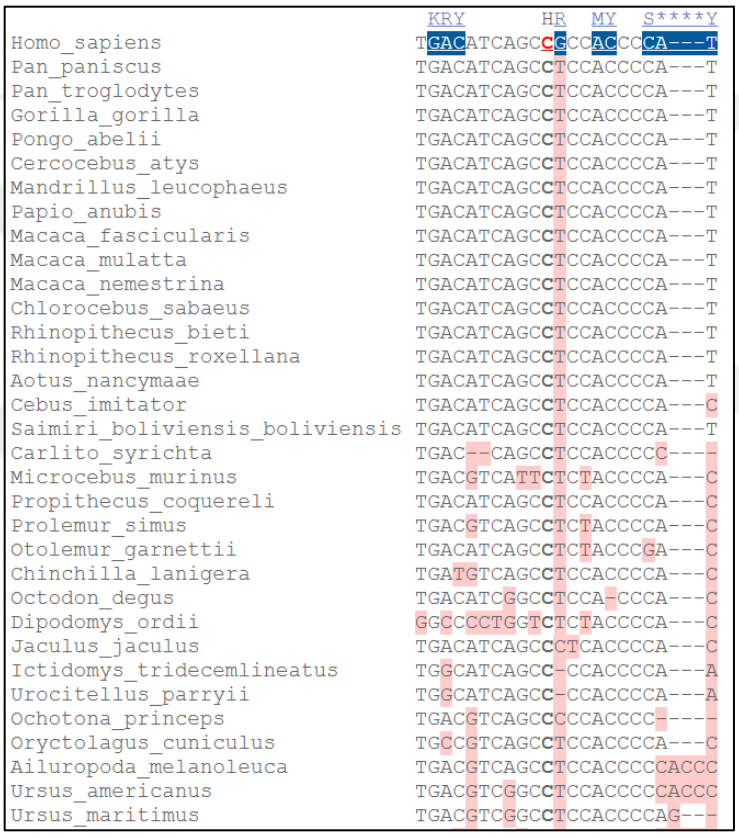


Figure 8. Evolutionary conserved region covering rs3026809

Multi-Species sequence alignment revealing site-specific conservation of rs3026809 (‘’C’’ marked in red). ‘’92 eutherian mammals EPO-Extended from Ensembl VEP’’ were selected. Only 33 species are shown here.

*ECE1* rs3026809 is closer to the ATF2 and CREB1 TF binding sites which may reflect the impact of this variant (Figure 9). Although introns do not code for proteins, they can contain regulatory elements like enhancers and TF binding sites. Additionally, variants in intronic regions can alter TF binding affinity, potentially

modulating gene expression (90). In case of *ECE1* rs3026809, CADD (Combined Annotation Dependent Depletion) Score is 14.48 which indicates moderate predicted deleteriousness. Additionally, LOEUF (Loss-of-Function Observed/Expected Upper Fraction) Score suggests that this gene has some tolerance to loss-of-function variation, having a score of 3.2100e-01.

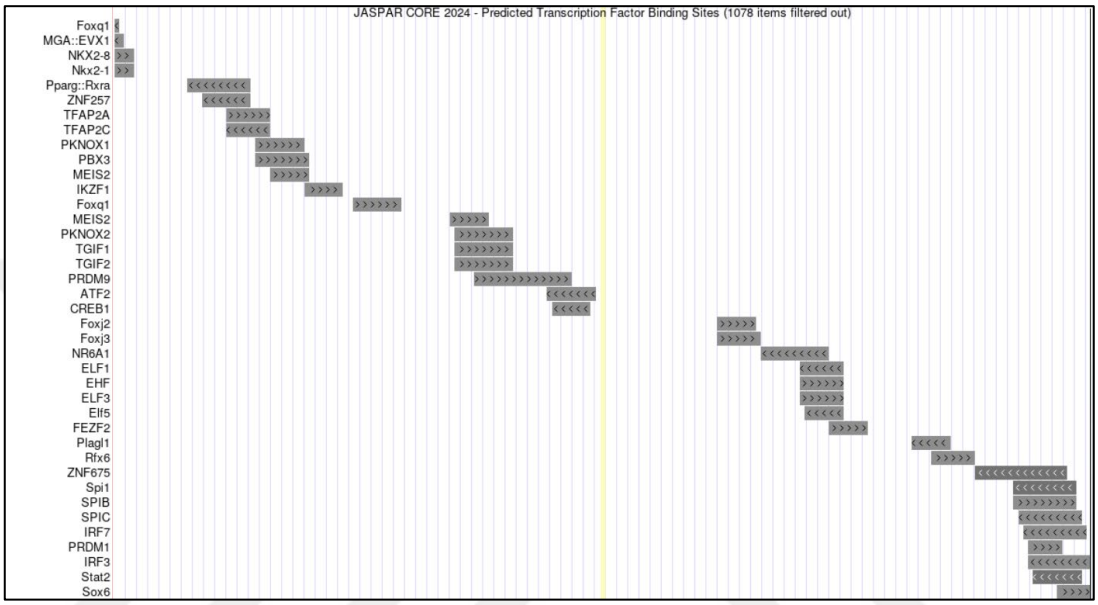


Figure 9. Predicted transcription factor binding sites of ECE1

Mapping of regulatory elements at the target locus, visualized using the JASPAR CORE 2024 database on the UCSC Genome Browser. The grey bars indicate estimated binding locations of different transcription factors. The yellow vertical highlight points to the exact site of the rs3026809 variant.

The normalized effect size (NES) for rs3026809 also suggested biological impact according to GTEX Portal. NES shows how much a genetic variant affects gene expression in different tissues. For rs3026809, score was 0.12 in nerve-tibial tissue so it is assumed that alternative allele may increase the gene expression. On the other hand, RegulomeDB score was 0.66, which means that the variant has moderate evidence of regulatory potential, possibly affecting TF Binding and chromatin accessibility.

## 4.4 Agarose Gel Electrophoresis of *ECE1* PCR Products

PCR was used to amplify the expected region covering rs3026809 in tumor and matched blood samples. The expected amplicon size was 368 bp (Figure 10). Following gel electrophoresis on a 2% agarose gel, all patient samples had sharp PCR bands of the expected size, indicating effective amplification. The negative control sample has no DNA band, indicating that PCR mixture has no contaminating DNA. Finally, to ensure the specific amplification of the target region and to eliminate non-specific bands, a second round PCR was performed under optimized conditions in some cases, and the resulting products were subsequently subjected to Sanger sequencing for confirmation.

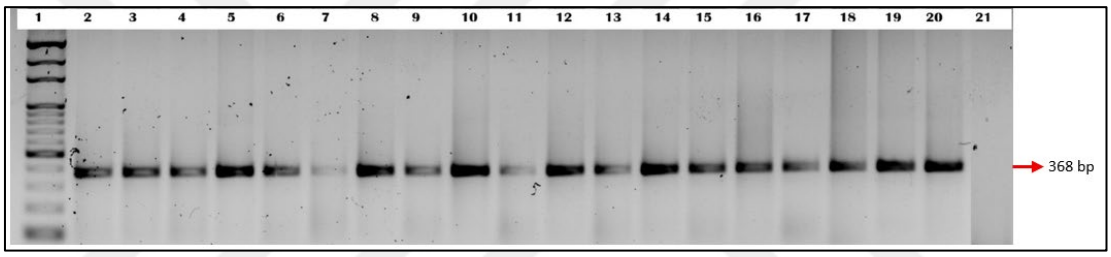


Figure 10. Analysis of *ECE1* PCR products

2% Agarose Gel. Lane 1:100 bp DNA ladder. Lanes 2–20 represent patient samples, band at the expected size of 368 bp (red arrow). Lane 21: negative control (2:T13-95/ 3:T12-46/ 4:T13-30/5:T14-146/6:T14-147/ 7:T13-1023/ 8:T13-03/ 9:T13-865/ 10: T12-18/ 11: T12-65/ 12: T14-34/ 13: T14-163/ 14: T13-708/ 15:T13-739/ 16:T13-606/ 17: T13-713/ 18:T13-716/ 19:T13-720/ 20: T13-821)

## 4.5 Analysis of *ECE1* rs3026809

Multi-step molecular analysis was carried out to evaluate the *ECE1* rs3026809 variant in our cohort. To ensure maximum precision; Sanger sequencing was performed as the gold-standard validation method, and AS-PCR and RFLP were preferred for the rapid determination of rs3026809 with various optimization steps. The results were then correlated with clinical parameters, to give a broad overview of the variant distribution among different subtypes of glioma.

### 4.5.1 Validation of *ECE1* rs3026809 by Sanger sequencing

Initially, Sanger sequencing was performed without using ExoSAP cleanup; however, the quality of the chromatograms was poor, with high background noise and unclear peak resolution. After that, ExoSAP cleanup was performed on the PCR products, and three samples were selected to be sequenced to obtain high-quality and clear chromatograms. Thus, based on the optimization, the same cleanup procedure was performed on the rest of the samples. The Sanger sequencing was successful for 19 out of 20 samples. The T13-720 sample had weak and noisy signals, possibly because of tumor heterogeneity. Sequence alignment revealed rs3026809 G>A. The overall accuracy was successful, producing high-quality chromatograms with clear and distinct peak resolution for each sample.

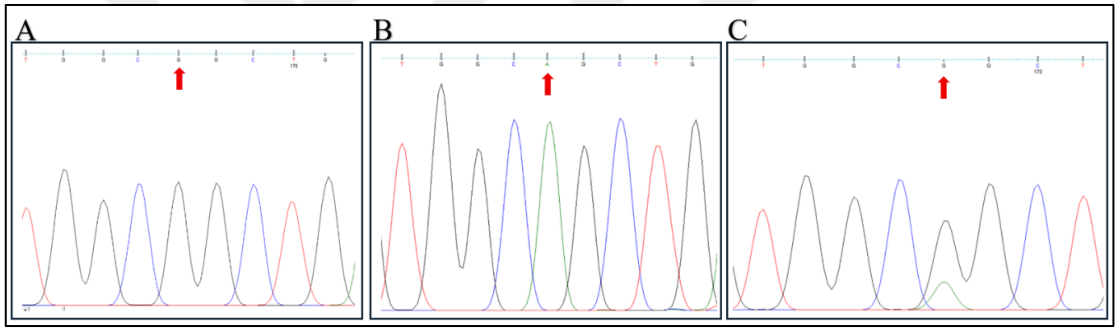


Figure 11. Sanger sequencing chromatograms of the rs3026809 variant

(**A**) T12-65: Wild-type genotype (G/G) (**B**) T12-46: Homozygous genotype (A/A) **(C)** T13-713: Heterozygous genotype (G/A); at the target SNP site (red arrow).

In Figure 11A–B, the Sanger sequencing results confirmed the targeted sequencing. The T12-65 tumor sample (Figure 11A) did not harbor the rs3026809 variant, whereas the T12-46 tumor sample (Figure 11B) carried the variant, demonstrating the expected G>A homozygote substitution. The patient sample with ID T13-713 (Figure 11C) exhibited a heterozygous state for the variant, which is consistent with the findings obtained from the AS-PCR analysis.

### 4.5.2 Detection of *ECE1* rs3026809 by Allele-specific PCR

AS-PCR was used to genotype the rs3026809 through both tumor and matched blood DNA samples (n=22). Results successfully distinguished the rs3026809 (G>A) genotypes based on differential amplification of the wild-type (G) and mutant (A) alleles. Two separate PCR reactions were performed for each sample, and clear, allele-specific amplification patterns were evaluated on 2.5% agarose gel electrophoresis (Figure 12). The expected 158bp amplicon was observed if the allele is present in the sample. Samples harboring the wild-type G allele displayed a distinct amplification band only in the reaction containing the WT primer, with no detectable product in the MUT primer reaction. Conversely, samples carrying the mutant A allele yielded a specific band exclusively in the reaction with the MUT forward primer. For heterozygous (G/A) samples, amplification bands were observed in both reactions, confirming the presence of both alleles. There were no bands in the negative control for both cocktails, indicating that the results were contamination free.

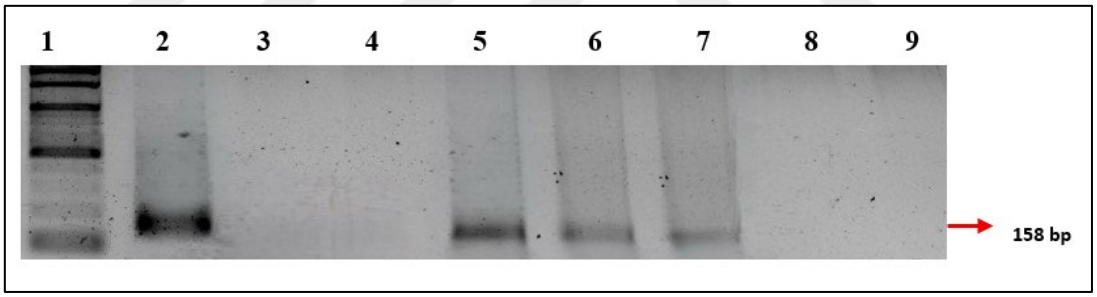


Figure 12. Genotyping of *ECE1* rs3026809 with AS-PCR

2.5% Agarose Gel. Lane 1:100 bp DNA ladder. Paired lanes for samples T12-65 (Lanes 2-3), T13-821 (Lanes 4-5), and T14-147 (Lanes 6-7). Lanes 8 and 9 serve as negative controls for the WT and MUT master mixes.

### 4.5.3 Detection of *ECE1* rs3026809 by RFLP

*CviKI*-1 is a type II restriction endonuclease that was isolated from the *Chlorella* virus NYs-1 is known for its ability to detect and cleave at sites RG'CY (where R = A or G and Y = C or T). Hence, *CviKI*-1 cuts the WT (G/G) in several parts of the 368 bp amplicon (Figure 13A). The expected band sizes are illustrated with the recognition sites for heterozygous, homozygous and WT genotypes in Figure 13B.

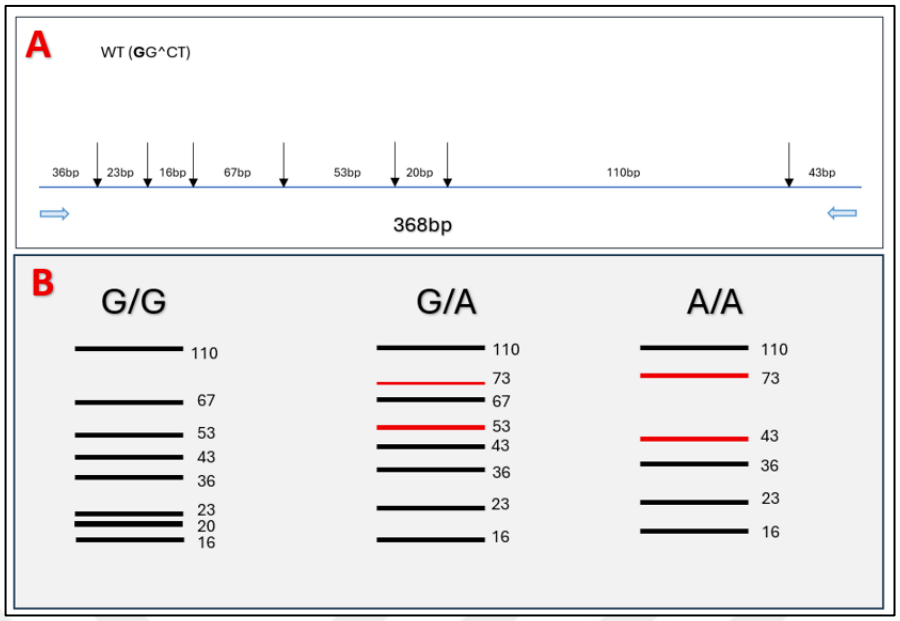


Figure 13. Expected RFLP digestion profiles for the *ECE1* rs3026809 variant

**(A)** Restriction enzyme recognition sites of the 368 bp *ECE1* PCR product with the *CviKI*-1 enzyme **(B)** Schematic illustration of the expected band patterns for the three genotypes.

Initial experiments to separate enzyme digestion products using 4% and 3% agarose gel electrophoresis (Figure 14 and Figure 15, respectively) did not yield satisfactory results for genotype calling. While larger-sized fragments 110 bp and 73 bp were distinguished, separation of smaller-sized products was not observed. To enhance better resolution, a composite gel matrix comprising 7% polyacrylamide and 0.6% agarose was used (Figure 16). However, this hybrid gel was insufficient for definitive allele determination, as the fragments remained poorly resolved. Furthermore, the indefinite DNA ladder in Figure 16B prevented the accurate size estimation of the digested fragments.

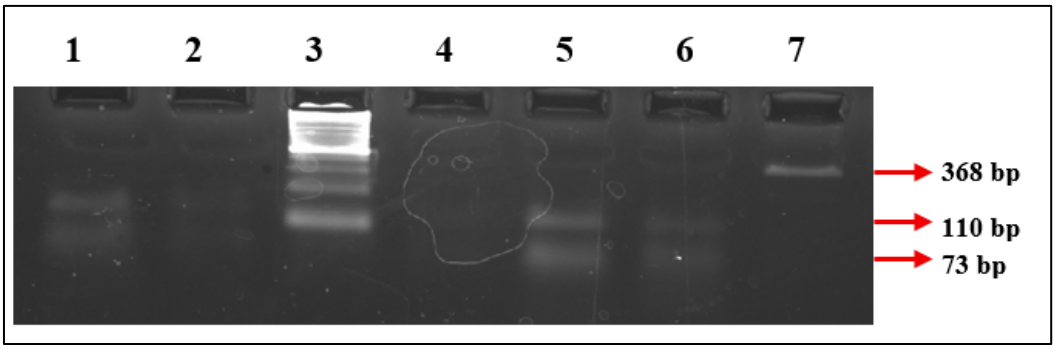


Figure 14. Separation of restriction fragments on a 4% agarose gel

Lane 1, 2, 4, 5 and 6 are patient samples (T13-95, B13-95, T12-46, B14-147, B14-163, respectively). Lane 3: 100 bp ladder. Lane 7: Undigested T12-65. While the 110 bp and 73 bp bands are seen, the smaller fragments are not clearly separated.

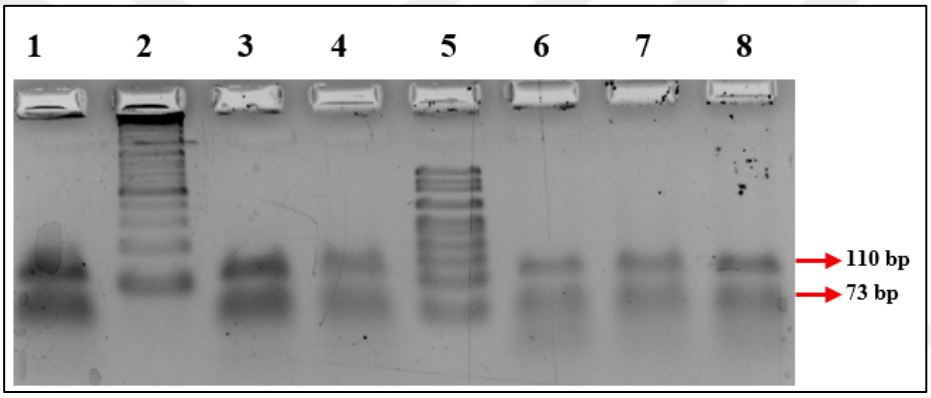


Figure 15. Separation of restriction fragments on a 3% agarose gel

Lane 1, 3, 4, 6, 7, and 8 are patient samples (T12-46, B14-147, T13-95, B13-95, B14-163, T12-65, respectively). Lane 2: 100 bp ladder. Lane 5: 50 bp ladder. While the 110 bp and 73 bp bands are seen, the smaller fragments are not clearly separated.

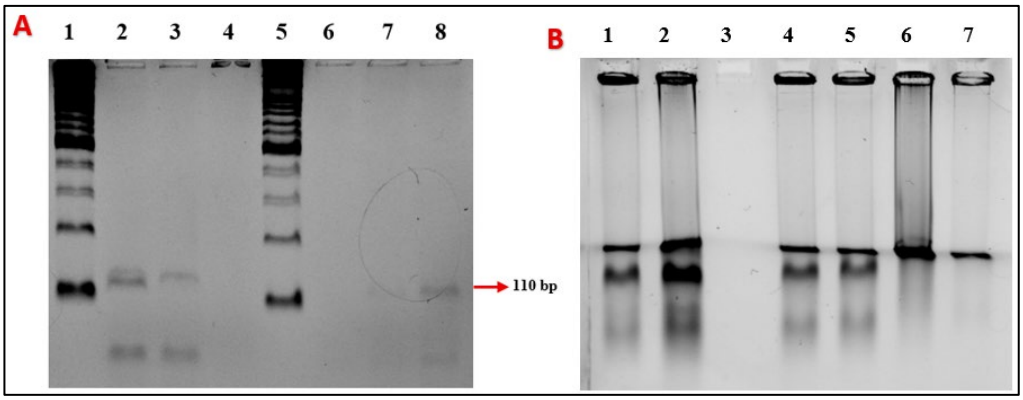


Figure 16. RFLP results of 7%Acrylamide+0.6% Agarose gel

**(A)** Although the 110 bp band is seen, smaller fragments are not visible. Lane 1 and 5 are 100 bp ladder. Lane 2, 3, 4, 6, 7, and 8 are patient samples (T12-46, B14-147, T13-95, B13-95, T12-65, B14-163, respectively). **(B)** Since DNA ladder is not visible, comments on fragments are not clearly done. Lane 3: 50 bp ladder. Lane 1, 2, 4, 5, 6, and 7 are patient samples (T13-716, B13-716, T13-720, B13-720, T13-821, B13-821, respectively).

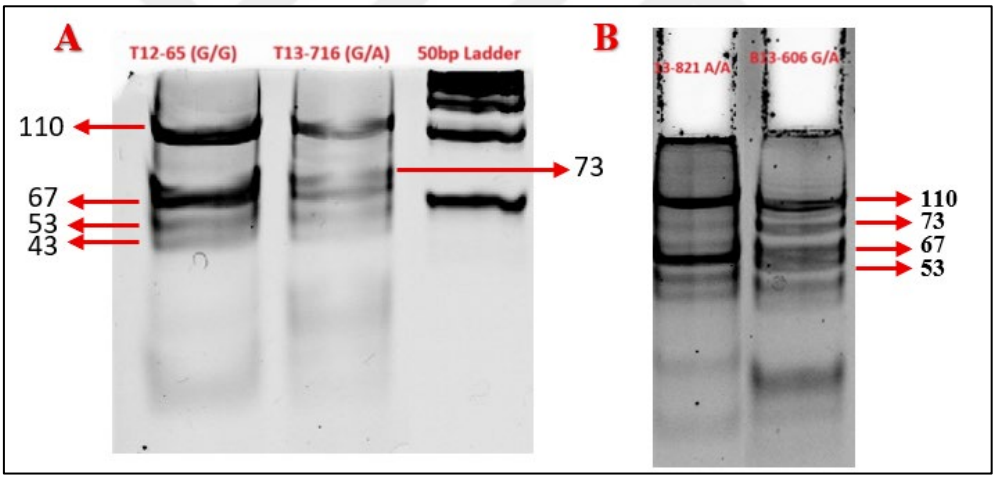


Figure 17. RFLP analysis of *ECE1* rs3026809 using 20% native PAGE

**(A)** High-resolution PAGE results showing the digestion profiles for the wild-type (G/G) (T12-65) and heterozygous (G/A) (T13-716) genotypes. **(B)** Analysis of the homozygous mutant (A/A) (T13-821) genotype and heterozygous (G/A) (B13-606) genotype. 50 bp ladder is used for size comparison.

Figure 17A shows 20% native PAGE gel of the G/G (wild-type) and G/A (heterozygous) genotypes after *CviKI*-1 digestion, confirming the fragment patterns predicted, illustrated in Figure 13A. However, even heterozygote genotype fragments are matched with the expected profile; homozygote genotype was not confirmed (Figure 17B).

The overall results of all samples genotyped are presented in Table 6. AS-PCR findings were consistent with Sanger sequencing results. However, for the T13-1023, AS-PCR result cannot be evaluated due to poorly resolved bands. On the other hand, RFLP analysis was performed only on the samples (n=13) presented in Figure 14-17. Because of the poor resolution and the detection rates, the remaining samples were not screened using this method; therefore, AS-PCR was preferred for all analysis.

Especially in grading of the gliomas, Ki-67 index has been an important tool. Definitive and precise Ki-67 determination requires an integrative method of comprehensive histopathological and molecular profiling analyses. The proliferative activity was assessed using Antigen Kiel 67 (Ki-67) index in all tumors via pathology department to detect the proliferative changes (91). All the patient-specific clinical outcome parameters, including relapse status and the molecular variations are listed (Table 6). Together with clinical and molecular background of dataset, statistical analysis in oligodendroglioma and GBM performed.

Table 6. Integrative analysis of clinical parameters and *ECE1* rs3026809 variant across glioma subtypes

| | | | | | | | | | | | | | | Sanger_Results | | ASPCR | |
|---|---|---|---|---|---|---|---|---|---|---|---|---|---|---|---|---|---|
| DNA ID | Grade | Age | Gender | Anatomic Location | 1p/19q status | ki67 | Relapse | Relapse_ki67 | mtDNA_Variation_Counts* | rs55705857 | *IDH1* | *TERT* | *ECE1_rs3026809* | *Blood* | *Tumor* | Blood | Tumor |
| 13-95 | Oligo2 | 46 | F | L-Frontal | co-deleted | 12% | - | - | ND | WT | R132H | C250T | MUT | G/A | G/A | G/A | G/A |
| 12-46 | Oligo2 | 31 | M | L-Frontal | co-deleted | 5% | - | - | 14 (6/14 same w/control) | A/G | R132H | C228T | MUT | ND | A/A | ND | A/A |
| 13-30 | Oligo2 | 40 | M | R-Lateral Sulcus | co-deleted | 3% | + | 14% | 14 (5/14 same w/control) | WT | R132H | C228T | MUT | A/A | A/A | A/A | A/A |
| 14-146 | Oligo2 | 28 | F | L-Frontal | co-deleted | 1% | + | 12% | ND | WT | R132H | C228T | MUT | ND | ND | G/A | G/A |
| 14-147 | Oligo2 | 44 | M | L-Frontal | co-deleted | 4% | - | - | ND | A/G | R132H | C228T | MUT | G/A | G/A | G/A | G/A |
| 14-177 | Oligo2 | 32 | M | L-Central | co-deleted | 8% | + | 22% | ND | WT | R132H | C250T | MUT | NS | NS | NS | NS |
| 13-1023 | Oligo3 | 37 | M | R-Frontal | co-deleted | 3% | - | - | ND | WT | R132H | C250T | MUT | ND | ND | G/A | NA |
| 13-03 | Oligo2 | 40 | M | R-Frontal | co-deleted | 2% | - | - | 30 (11/30 same w/control) | WT | R132H | C228T | WT | ND | ND | ND | G/G |
| 13-865 | Oligo2 | 38 | M | R-Frontaperiatal | co-deleted | NA | + | 25% | ND | WT | R132H | C250T | WT | ND | ND | ND | G/G |
| 12-18 | Oligo2 | 29 | M | L-Frontal | co-deleted | 3% | + | 17% | ND | WT | R132H | C250T | WT | ND | G/G | ND | G/G |
| 12-65 | Oligo2 | 39 | M | L-Temporal | co-deleted | 1% | - | - | 16 (7/16 same w/control) | A/G | R132H | C228T | WT | ND | G/G | ND | G/G |
| 14-34 | Oligo3 | 47 | M | R-Occipital | co-deleted | 5% | + | 15% | ND | A/G | R132H | C228T | WT | ND | ND | ND | G/G |
| 14-163 | Oligo3 | 35 | F | L- Posterior Temporal | co-deleted | 15% | - | - | ND | WT | R132H | C228T | WT | G/A | G/G | ND | G/G |
| 13-708 | Oligo3 | 28 | F | L- Posterior Frontal | co-deleted | 4% | - | - | 3 (1/3 same w/control) | A/G | R132H | C228T | WT | ND | ND | ND | G/G |
| 13-739 | Oligo3 | 31 | F | L-Frontal | co-deleted | 10% | - | - | ND | WT | R132H | C228T | WT | ND | ND | ND | G/G |
| 14-195 | Control | 27 | M | Temporal Tissue | not | - | - | - | ND | WT | WT | WT | WT | ND | ND | ND | ND |
| 13-606 | GBM | 67 | M | R-Frontal | not | 10% | - | - | ND | WT | WT | C228T | ND | ND | G/A | G/A | G/A |
| 13-713 | GBM | 78 | F | Cerebellum | not | 8% | - | - | ND | WT | WT | C250T | ND | ND | G/A | G/A | G/A |
| 12-54 | GBM | 54 | M | L-Occipital | not | 8% | - | - | ND | WT | WT | C228T | ND | ND | G/A | G/A | G/A |
| 12-75 | GBM | 56 | F | R-Frontal | not | 35% | + | NA | ND | WT | WT | C228T | ND | ND | ND | G/A | G/A |
| 12-102 | GBM | 56 | M | R-Occipital | not | 10% | + | NA | ND | WT | WT | C250T | ND | ND | ND | G/A | G/A |
| 12-105 | GBM | 44 | M | R-Periatal | not | 60% | + | 14% | ND | WT | WT | C228T | ND | ND | ND | G/A | G/A |
| 13-716 | GBM | 64 | F | L-Frontal | not | 30% | + | NA | ND | WT | WT | C228T | ND | G/A | G/A | G/A | G/A |
| 13-720 | GBM | 56 | M | R-Temporal | not | 6% | + | NA | ND | WT | WT | C250T | ND | A/A | NA | A/A | A/A |
| 13-821 | GBM | 63 | F | L-Occipital | not | 30% | + | NA | ND | WT | WT | C228T | ND | G/A | A/A | G/A | A/A |

Clinical and molecular characteristics of the patient cohort, categorized by tumor type summarized including age, gender, anatomic location, and molecular markers.

* *NS: No Sample NA: Not Available ND: Not Done*

### 4.6 Statistical Analysis

All statistical analysis was performed with identified variant and clinical data through JAMOVİ. The Ki-67 proliferation index was compared between GBM and oligodendroglioma tumors in all patients and significant association was observed which was considerably higher in GBM than in oligodendroglioma ($p = 0.002$). Fisher's exact test revealed no significant associations between tumor type (GBM vs. oligodendroglioma) and; anatomic tumor location ($p = 0.10$) or gender ($p = 0.678$). On the other hand, oligodendrogliomas were most frequently observed in the left frontal region (29.2%), whereas GBM cases showed no clear regional predominance, with equal representation in the right frontal (8.3%) and left occipital (8.3%) regions.

The *ECE1* rs3026809 (G>A) variant is present in 100% of GBM patients (9/9), 60% of Oligo2 (6/10), and 20% of Oligo3 patients (1/5). Considering all 24 patient samples, a significant association ($\chi^2$ test, $p= 0.0082$) was observed between tumor grade and *ECE1* variant status. The presence of the variant was not correlated ($p=0.173$) with Ki67 index. Notably, a significant difference in age was observed between patients with the *ECE1* variant and those with the WT allele ($p = 0.02$), indicating an association between variant and age in our cohort.

Table 7**.** Pairwise Fisher's Exact Test Analysis Among Patient Groups with *ECE1* Variant

| **Comparison** | **Group 1 MUT** | **Group 2 MUT** | **Odds Ratio (OR)** | **p-value** | **Significance** |
|---|---|---|---|---|---|
| **Oligo2 vs GBM** | 6/10 (60%) | 9/9 (100%) | 0.0760* | p=0.087 | ☆ Borderline trend |
| **Oligo3 vs GBM** | 1/5 (20%) | 9/9 (100%) | 0.0175* | **p=0.005 **** | ★ Significant |
| **All Oligos vs GBM** | 7/15 (47%) | 9/9 (100%) | 21.5* | **p=0.009 **** | ★ Significant |
| **Oligo2 vs Oligo3** | 6/10 (60%) | 1/5 (20%) | 6.00 | p=0.282 | Not significant |

Analysis of pairwise statistical comparisons assessing the frequency of the *ECE1* rs3026809 variant between different glial tumor groups

*Haldane-Anscombe correction applied

Pairwise Fisher's Exact Test analysis among patient groups with *ECE1* variant is summarized in Table 7. Pairwise comparisons indicated a non-significant trend towards Oligo2 relative to GBM (p = 0.087), while Oligo3 exhibited statistically significant association with GBM (p= 0.005). However, Oligo 2 vs Oligo 3 showed no association (p=0.282). On the other hand, when all Oligo grades were compared with GBM, significant association was observed (p= 0.009). This strongly supports the hypothesis that this variant may contribute to malignant progression or may be a molecular marker of aggressive glioma.

The genotype distribution across all gliomas does not deviate significantly from Hardy-Weinberg Equilibrium (p=0.8887) as represented in Table 8, suggesting that rs3026809 G>A is most likely a germline SNP rather than a recurrent somatic mutation. In addition, blood-tumor concordance reached 84.2 % through all patients (except two samples:14-163 and 13-821), screened via Sanger/AS-PCR. The patient blood sample B13-821 showed G/A genotype however, tumor sample T13-821 (A/A) exhibited a classic loss of heterozygosity (LOH) of WT G allele, suggesting that this variant may actually confer growth advantage in the tumor. In contrast, patient tumor sample T14-163 (G/G) showed discordant pattern with the blood sample B14-163 (G/A). Both AS-PCR and Sanger results are consistent with these two findings.

Table 8**.** Hardy-Weinberg Equilibrium (HWE) of *ECE1* rs3026809

| | **G/G (obs/exp)** | **G/A (obs/exp)** | **A/A (obs/exp)** | **A freq (q)** | **HWE p-value** |
|---|---|---|---|---|---|
| **All gliomas** | 8/8.2 | 12/11.7 | 4/4.2 | 0.417 | p=0.8887 |

Statistical assessment of the Hardy-Weinberg Equilibrium for the *ECE1* rs3026809 variant throughout the total patient cohort.

The Ki67 index is well-established immunohistochemical marker of the tumor proliferative activity and correlated with glioma grades (92). Binomial logistic regression was performed to evaluate the association between *ECE1* variant status and Ki67 proliferation index plus tumor grade. The model demonstrated an overall classification accuracy of 0.905 (90.5%) and an AUC of 0.969 (Figure 18). However, these results should be interpreted cautiously due to the small sample size (n=24).

| Observed | MUT | WT | % Correct |
|---|---|---|---|
| MUT | 13 | 1 | 92.9 |
| WT | 1 | 6 | 85.7 |

*Note.* The cut-off value is set to 0.5

Predictive Measures

| Accuracy | AUC |
|---|---|
| 0.905 | 0.969 |

*Note.* The cut-off value is set to 0.5

Figure 18. Binomial logistic regression analysis of *ECE1* rs3026809 status, Ki67 index and tumor grade

The top panel illustrates the classification matrix, including observed versus predicted values for the MUT and WT genotypes. The model achieved an overall accuracy of 0.905 (90.5%).

### 4.7 *ECE1* and rs3026809 From COSMIC and ClinVar

COSMIC and ClinVar were used to analyze the *ECE1* and specifically rs3026809 variant. The results showed only one somatic missense substitution entry for *ECE1* in the central nervous system, specifically in gliomas (c.1337G>T; p.S446I; COSM3966256). On the other hand, there were 161 germline variants for *ECE1* reported in ClinVar, with missense variants accounting for the majority (n = 117), followed by splice site (n = 5) and UTR variants (n = 5). Most of the variants (n=104) were classified as variants of uncertain significance (VUS). The rs3026809 was not submitted in either the COSMIC or ClinVar databases.

## 4.8 RNAseq and DeSeq2 Analysis

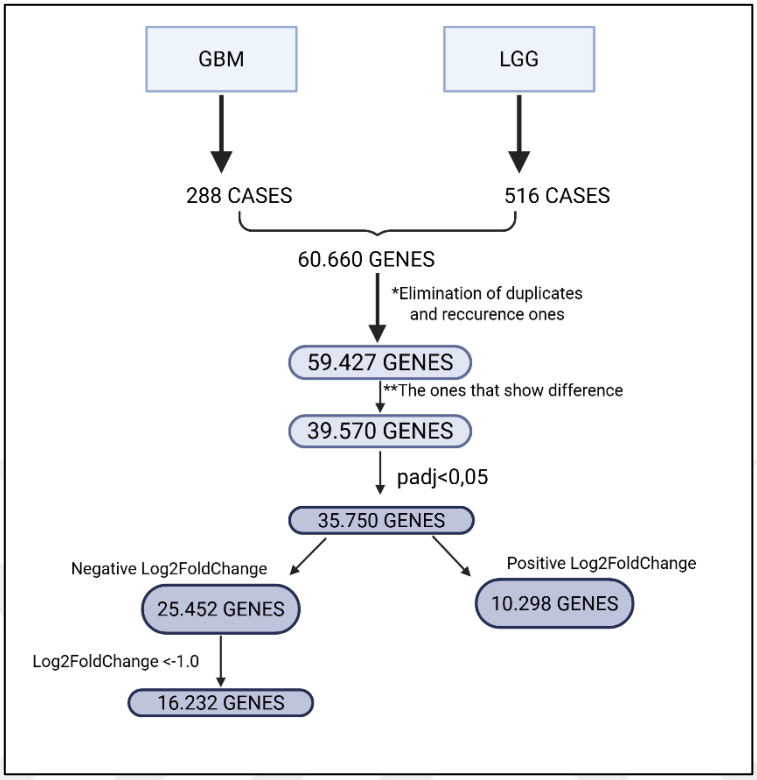


Figure 19. RNAseq and DESeq2 analysis for GBM vs LGG

Pipeline representing the systematic filtering process used to compare glioblastoma (GBM, n=288) and low-grade glioma (LGG, n=516) cases retrieved from TCGA.

Figure 19 illustrates the workflow to identify differentially expressed genes in LGG and GBM using TCGA RNA sequencing data. 288 cases for GBM and 516 cases for LGG were merged and yielded a raw set of 60,660 genes. After filtering duplicates, 59,427 genes were used in main analysis. Each dataset was processed using DESeq2 R package to compare the gene expression profiles among LGG and GBM. The package compares cohorts based on ‘’B to A conditions’’. Therefore, LGG was designated as condition B and GBM as condition A. The resultant positive log2FoldChange indicates the higher, whereas negative log2FoldChange indicates the lower gene expression in LGG compared to GBM.

This analysis successfully identified a total of 39,570 genes that exhibit differences in expression between the two glioma subtypes. By filtering out by the padj

<0.05, 35,750 genes have been revealed. Furthermore, the comparison of LGG vs GBM indicated that:

- 25,452 genes had higher expression in GBM compared to LGG (Negative log2FoldChange scores). To obtain a specific set of genes, log2foldchange cut-off was applied (<-1.0) resulting in 16,232 genes.

- 10,298 genes had higher expression in LGG compared to GBM (Positive log2FoldChange scores).

This final set of differentially expressed genes represents the robust molecular signature distinguishing these two glioma types.

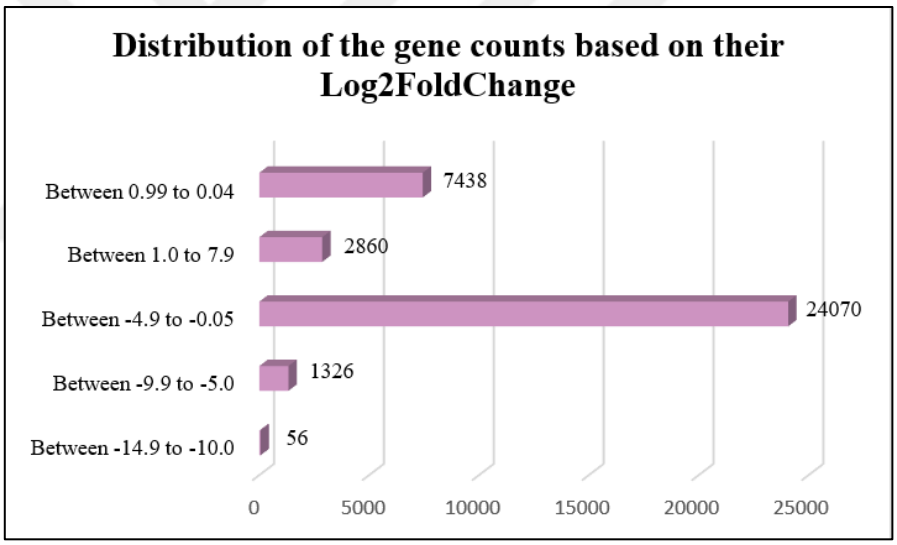


Figure 20**.** Distribution of 35,750 differentially expressed genes according to Log2 fold changes intervals

Genes were grouped based on fold change levels, with Log2 fold change intervals represented on the y-axis and gene counts on the x-axis.

Figure 20 highlights 56 genes (0.1%) with the most significantly upregulated in GBM compared to LGG, determined by Log2 fold change analysis. Overall, these genes share a common aggressive growth signature, with most involved in cell growth and division. For instance; *H3C7*, *H4C6*, and *H2BC10* are core histones that are highly expressed during DNA replication to support nucleosome assembly, chromatin

formation and genome stability. In addition, most of the genes consist of functional RNAs. On the other hand, many genes that end with 'P' (e.g., *RN7SKP255*, *RN7SL166P*) are pseudogenes, known as fossil copies of genes, that lost their function over evolution.

After the identification of the differentially expressed genes in GBM, PPI network analysis was performed using the Search Tool for the Retrieval of Interacting Genes/Proteins (STRING) database, to visualize functional associations. The distinct sets were interpreted to pinpoint the most significantly enriched and relevant biological pathways that may potentially drive the differences observed between the two glioma subtypes.

The first enrichment plot (Figure 21) shows that genes upregulated in GBM relative to LGG are strongly enriched in immune system–related biological processes, suggesting a robust activation of inflammatory and immunoregulatory pathways. This is consistent with the well-known highly inflammatory microenvironment of GBM, characterized by increased infiltration of tumor-associated macrophages/microglia, elevated cytokine and chemokine production, and enhanced expression of immune checkpoint molecules. Moreover, the defense response enrichment indicates that, GBM is transcriptionally adapted to high cellular stress, likely due to hypoxia, metabolic pressure, DNA damage responses, pro-inflammatory signaling (93).

On the other hand, the second enrichment plot (Figure 22) shows that genes downregulated in GBM relative to LGG are most strongly enriched in neuronal development and synaptic signaling pathways. Processes such as synaptic signaling, chemical synaptic transmission, trans-synaptic signaling, and regulation of synaptic plasticity are significantly reduced in GBM. These processes indicate that GBM tumors have reduced expression of genes in neuronal communication and mature synaptic structure, which are relatively more preserved in LGG.

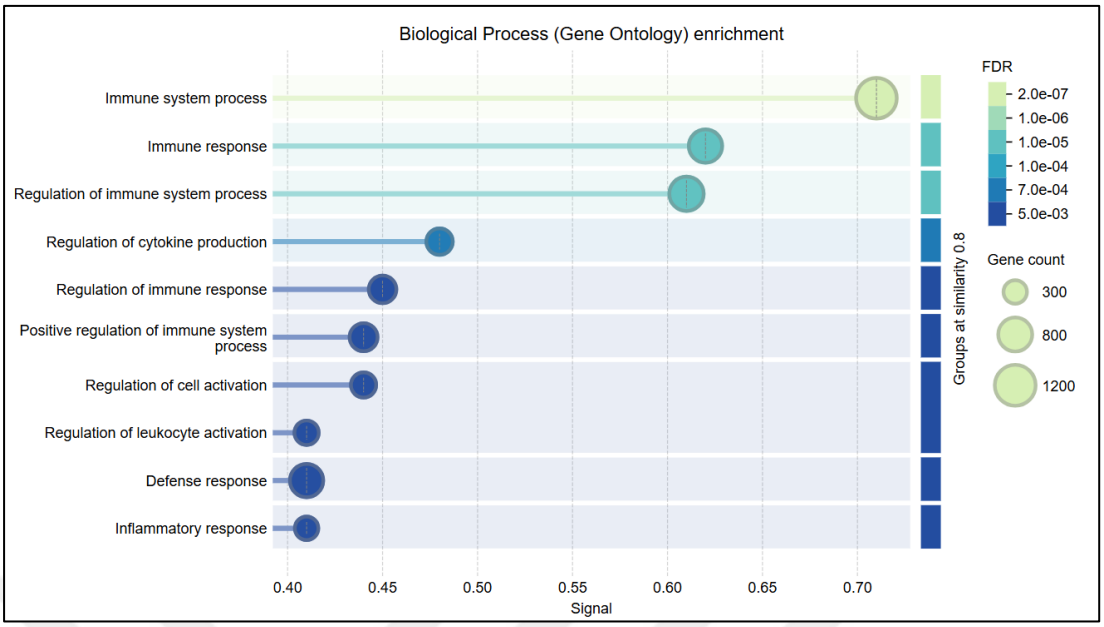


Figure 21. Gene Ontology (GO) enrichment for upregulated genes in GBM

The x-axis represents the enrichment signal, and bubble size indicates the number of genes associated with each process. Bubble color represents the False Discovery Rate (FDR). Mainly robust activation of immune system processes was observed (Negative log2FoldChange in DESeq2 Analysis).

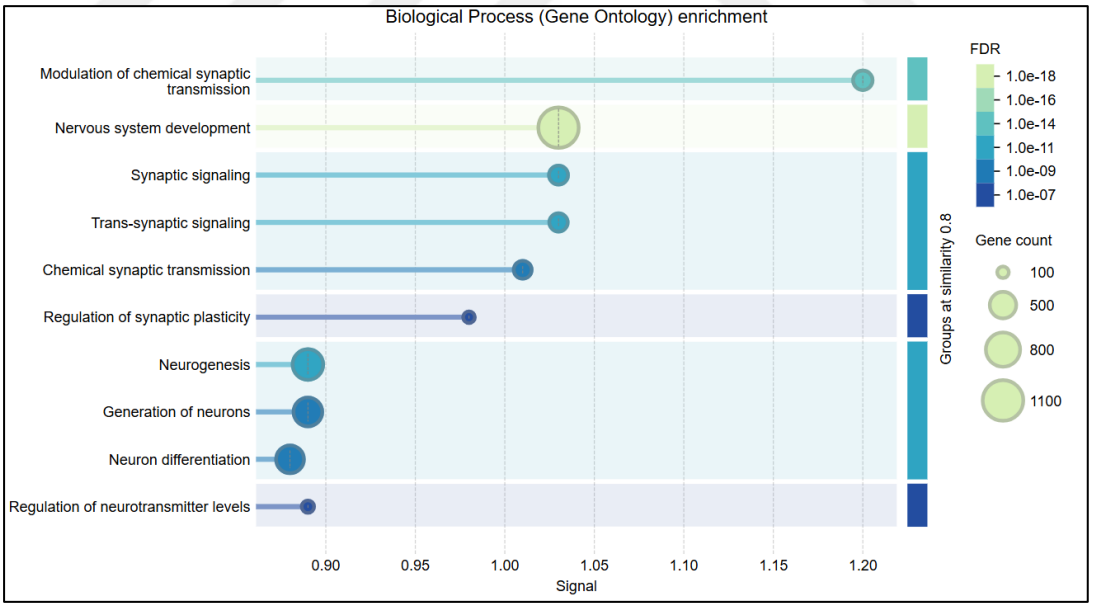


Figure 22. Gene Ontology (GO) enrichment of downregulated genes in GBM.

The x-axis represents the enrichment signal, and bubble size indicates the number of genes associated with each process. Crucial enrichment in nervous system development, synaptic signaling and neurotransmitter regulation was observed (Positive log2FoldChange in DESeq2 Analysis)

Table 9**.** DESeq2 analysis for *ECE1*

| | baseMean | log2FoldChange | lfcSE* | Stat* | pvalue | padj |
|---|---|---|---|---|---|---|
| ***ECE1*** | 6619,901113 | -0,717880973 | 0,059841026 | -11,99646842 | 3,71E-33 | 8,41E-33 |

Differential expression metrics for *ECE1* retrieved from the comparative transcriptomics of LGG and GBM TCGA cohorts.
*lfcSE (Log Fold Change Standard Error) / stat (The Wald Statistic)

*ECE1* is included in the largest group of differentially expressed genes (26,043 genes) spanning from -4.9 to ~0 (Figure 20). In DESeq2 analysis (Table 9), the log2FoldChange value for *ECE1* is -0.717880973. The negative fold change indicates that *ECE1* is significantly upregulated in GBM compared to LGG, or conversely, downregulated in the reference condition (LGG) relative to GBM. Furthermore, the average normalized count (baseMean) of the *ECE1* across all samples is 6619.90113, suggesting robust expression. Crucially, the analysis yields a highly statistically significant result (p-value= 3.71E-33 and padj= 8.41E-33) confirming that the observed difference is not due to random chance. Therefore, *ECE1* could be a significant biomarker that is expressed at substantially higher levels in GBM compared to LGG.

### 4.9 PPI Network Analysis

PPI network analysis and intersection analysis revealed that Endothelin (EDN)-*EDN1, EDN2, EDN3,* Angiotensinogen *(AGT),* Solute Carrier Family 9 Member A1 *(SLC9A1),* Calcitonin Related Polypeptide Alpha *(CALCA),* Kell Metallo-Endopeptidase *(KEL), ECE1* and *ECE2* are closely related genes. Subsequent analyses were performed to assess the ability of these nine genes to differentiate GBM from LGG. For each gene, case IDs and coding and noncoding variants, as well as CNVs, were retrieved from TCGA (Table 10). Chromosomal locations of genes revealed that only *SLC9A1* was located on 1p whereas no genes were identified on 19q among the TCGA-GBM and LGG datasets. The majority of the identified variants were missense, while nonsense, silent, intronic, and noncoding variants were observed at lower frequencies. Interestingly, a non-coding exonic variant in *CALCA*, located on chromosome 11 (exon 5) was identified. The VEP impact score classified this variant as a modifier. It has been previously reported in ClinVar as VUS with a very low allele

frequency (f = 0.0000369). In addition, an intronic variant in *ECE2*, located on chromosome 3 (intron 2) was defined. This variant has not been reported in ClinVar, is similarly classified as a modifier by VEP with an extremely low allele frequency (f = 0.0000029).

The presence of these genes was further evaluated in our research group's targeted sequencing data (Table 11). With the exception of *EDN2*, all genes were also detected in our cohort. Notably, targeted region was 1p/19q and stringent filtering strategy was applied in sequencing analysis to eliminate the default variants in other chromosomes. Therefore, no detailed investigation was performed in the genes that are out of our research scope. Only *SLC9A1* was identified within the targeted region (1p) harboring rs3738689 C>G. Additionally, *AGT* was also located on chromosome 1 but on q arm, hence out of targeted locus. Even though in our cohort the same genes were identified reported in PPI network analysis, only *SLC9A1* was evaluated. The remaining genes may be considered in future studies.

Table 10. Variations and CNV profiles of ECE1-associated genes identified by PPI analysis

| Gene_Name & Chromosome | Tumor_Type | Case_ID | Variant | CNV_count |
|---|---|---|---|---|
| EDN3_chr20 | GBM | TCGA-06-5416 | C159 SILENT | 176 |
| | LGG | - | - | 42 |
| EDN2_chr1 | GBM | - | - | 57 |
| | LGG | TCGA-DU-5854 | R87C MISSENSE | 189 |
| CALCA_chr11 | GBM | TCGA-19-1386 | R131H MISSENSE | 69 |
| | | TCGA-76-4925 | E46K MISSENSE | |
| | | TCGA-12-1600 | C>T NONCODING | |
| | LGG | - | - | 81 |
| EDN1_chr6 | GBM | - | - | 65 |
| | LGG | TCGA-S9-A7J2 | S179 SILENT | 40 |
| AGT_chr1 | GBM | TCGA-06-5416 | G260E MISSENSE | 76 |
| | | TCGA-06-5416 | P481 SILENT | |
| | | TCGA-06-5416 | K169 SILENT | |
| | | TCGA-14-1396 | L359I MISSENSE | |
| | LGG | TCGA-DU-6392 | K287N MISSENSE | 39 |
| | | TCGA-DU-6392 | A150S MISSENSE | |
| | | TCGA-VM-A8CF | V233 SILENT | |
| SLC9A1_chr1 | GBM | TCGA-06-5416 | R669W MISSENSE | 72 |
| | | TCGA-06-5416 | D95N MISSENSE | |
| | | TCGA-19-1787 | I719 SILENT | |
| | LGG | TCGA-DU-6392 | Q815 SILENT | 198 |
| | | TCGA-DU-6392 | D755 SILENT | |
| | | TCGA-HT-7873 | G150 SILENT | |
| ECE2_chr3 | GBM | TCGA-06-0190 | C>T INTRON | 78 |
| | LGG | - | - | 39 |
| KEL_chr7 | GBM | TCGA-06-0192 | X75 SPLICE | 412 |
| | | TCGA-06-5414 | X28 SPLICE | |
| | | TCGA-06-5415 | X75 SPLICE | |
| | | TCGA-06-5416 | I246 SPLICE REGION | |
| | | TCGA-06-5416 | R192Q MISSENSE | |
| | | TCGA-06-0145 | V336M MISSENSE | |
| | | TCGA-06-0152 | S187Y MISSENSE | |
| | | TCGA-06-0238 | R47W MISSENSE | |
| | | TCGA-06-0879 | P400H MISSENSE | |
| | | TCGA-06-2563 | G368V MISSENSE | |
| | | TCGA-06-5408 | K308R MISSENSE | |
| | | TCGA-12-1599 | R428H MISSENSE | |
| | | TCGA-41-2572 | R655W MISSENSE | |
| | LGG | TCGA-FG-A87Q | Y253* NONSENSE | 164 |
| | | TCGA-P5-A5EX | R700* NONSENSE | |
| | | TCGA-DU-6392 | P559L MISSENSE | |
| | | TCGA-DU-7007 | R192Q MISSENSE | |
| | | TCGA-FG-6692 | R180C MISSENSE | |
| | | TCGA-HT-7690 | L55W MISSENSE | |
| | | TCGA-HT-7860 | R14C MISSENSE | |
| | | TCGA-QH-A6XC | S25I MISSENSE | |
| | | TCGA-S9-A6TX | V639I MISSENSE | |

Genes associated with *ECE1* were identified using TCGA data, and the corresponding case IDs with specific variants are presented. All data were retrieved from the TCGA LGG (TCGA-LGG) and GBM (TCGA-GBM) cohorts (dbGaP Study Accession: phs000178).

Table 11. Assessment of PPI-network genes within the targeted sequencing cohort

| Patient_ID | Gene_and_Variant | Chromosome | Exonic/Intronic | Allele_Frequency |
|---|---|---|---|---|
| 12-18 | CALCA rs2644690 (G>A) | Chr11 | exon1 | 0.986 |
| 13-03 | CALCA rs2644690 (G>A) | Chr11 | exon1 | 0.986 |
| 13-95 | CALCA rs2644690 (G>A) | Chr11 | exon1 | 0.986 |
| 13-739 | CALCA rs2644690 (G>A) | Chr11 | exon1 | 0.986 |
| 13-708 | CALCA rs2644690 (G>A) | Chr11 | exon1 | 0.986 |
| 13-1023 | SLC9A1 rs3738689 (C>G) | Chr1 | intron | 0.306 |
| 14-34 | EDN3 rs197178 (A>T) | Chr20 | intron | 0.298 |
| | CALCA rs2644690 (G>A) | Chr11 | exon1 | 0.986 |
| | EDN1 rs2747708 (C>G) | Chr6 | intron | 0.400 |
| | EDN1 rs56214323 (delCG) | Chr6 | intron | 0.0000109 |
| | EDN1 rs66904955 | Chr6 | NA | NA |
| | KEL rs3757853 (C>G) | Chr7 | exon9 | 0.670 |
| 12-46 | CALCA rs2644690 (G>A) | Chr11 | exon1 | 0.986 |
| | ECE2 rs843351 (T>C) | Chr3 | intron | 0.919 |
| | KEL rs8176044 (T>C) | Chr7 | intron | NA |
| 14-147 | CALCA rs2644690 (G>A) | Chr11 | exon1 | 0.986 |
| | AGT rs7080 (T>C) | Chr1 | exon3 | 0.947 |
| 14-195_control | CALCA rs2644690 (G>A) | Chr11 | exon1 | 0.986 |
| | AGT rs2478543 (T>C) | Chr1 | intron | 0.577 |
| 14-163 | CALCA rs2644690 (G>A) | Chr11 | exon1 | 0.986 |
| | ECE2 rs34745735 (delTTTT) | Chr3 | intron | 0.520 |
| | ECE2 rs1387976 (C>A) | Chr3 | intron | NA |

The presence of genes identified through PPI analysis within our research group's targeted sequencing data. Variants located within the defined target region are highlighted.

# 5 DISCUSSION

Comprehending genomic variation in gliomas, especially in the context of integrating molecular findings with clinical needs, has become increasingly essential. Here, variants are discussed that may not be the main driving factor, but may nonetheless have an effect on tumor behavior, progression or heterogeneity. The study focused consequently on detecting changes that could have a regulatory effect and be related to disease dynamics.

Among the filtered candidates in our targeted sequencing dataset, *ECE1* emerged as the most compelling gene to investigate further, primarily because of its significant involvement in glial tumor biology recently. Several independent studies published within the last few years have highlighted the roles of *ECE1* in extracellular matrix dynamics, glial cell signaling, angiogenic modulation, and stress-response pathways—all processes that are increasingly recognized as central to oligodendroglial tumor behavior. This growing body of evidence placed *ECE1* at the intersection of pathways highly relevant to our research focus. The identification of rs3026809-potential regulatory variant- near predicted TF binding sites supports the relevance of a gene already implicated in glial tumor mechanisms. Thus, the selection of *ECE1* was not arbitrary, but grounded in a classical triad of selection criteria used in molecular oncology: 1) biological relevance, 2) evidence of regulatory influence, and 3) alignment with emerging scientific consensus. In this context, choosing *ECE1* as the gene of interest reflects both the structure of the data and the direction of current research, positioning the variant within a framework of scientifically justified significance.

The biosynthesis of ET-1 is highly essential for the function and activation of ECE1. Initially, ET-1 was produced as pre-pro-ET-1 (212 amino acids), which is cleaved by PC7 convertases to generate Big ET-1 (39 amino acids). ECE1 then facilitates the important final step by splitting Big ET-1 into two products: the active ET-1 (21 amino acids), a powerful vasoconstrictor, and the C-terminal fragment (CTF), whose role in this pathway remains unknown. Since ET1 has short half-life (90s) its biological effects are completely dependent on its enzymatic activation of

ECE1. As a result, this process highlights the significance of ECE1 in the ET-1 system, as it directly influences the availability of active ET-1, which is vital for vascular homeostasis, blood pressure regulation, and pathological conditions such as hypertension and cardiovascular diseases (94). According to a recent study aiming to analyze GBM malignant cell lineage pseudotime trajectories, *ECE1* was observed to be upregulated in the early phases of GBM, with its highest abundance in pseudotime state-1 cells (95). On the other hand, analysis of GBM in different stages revealed that *ECE1* and *KAZN* were overexpressed in GBM1 (early phase), while *ID3, PARK7, RPL11*, and *STMN1* genes were generally expressed in late phase.

*ECE1* variants were searched throughout the GBM and LGG in TCGA database and 2 missense variations (L186F and G116D) in 2 different GBM patients (TCGA-12-1598 and TCGA-19-5956) were observed. In TCGA sample 12-1598, genes harboring missense mutations—specifically *SUSD4, FUT3, NPB, NNT*, and PCOLCE2—demonstrate functional interactions with *ECE1*, collectively serving as critical regulators of cellular and extracellular homeostasis. In the TCGA-19-5956 sample, a few more variations were identified. In general, those genes are dedicated to the structural integrity of cells- for instance *SPTA1, LAMC1, PKP1, FBN3* etc.; innate and adaptive immune response- *NLRP9, FCGR2C*, *SIGLEC9* etc.; and role in signal transduction- *WNT3A, TGFB2, JAK1, PIK3CD* etc. Additionally, two missense variations located in the catalytic domain of ECE1c, observed in both patients have been previously discussed in the literature and linked to GBM (63). Besides these, several CNV's (gain, amplification, homozygous & heterozygous deletion) were reported in these patients.

A curious phenomenon arising in our cohort is 8/16 tumors contain mutant rs3026809, localized in the left hemisphere. The left frontal lobe harbors high number of oligodendroglial precursor cells (OPCs), which are suggested to be the cells of origin for the *IDH*-mutant and 1p/19q co-deleted oligodendroglioma (96). First of all, minor regulatory changes, particularly those located around transcription-factor binding motifs, including rs3026809, may alter the baseline gene expression threshold in these progenitor cells, thereby predisposing certain microenvironments to neoplastic transformation. Second, recent neurodevelopmental evidence implies that

transcriptional landscapes and epigenetic maturation patterns are predominantly localized in left frontal lobe, especially in areas that regulate language, executive and high-order integration with all (97). Third, *ECE1* harboring rs3026809 has been implicated in cellular stress responses, extracellular matrix reorganization, and glial signaling which also differ regionally across the cortex and may modulate OPCs to oncogenic stimuli (97, 98). Lastly, the recurrent detection of the rs3026809-A in many patients with in the left-frontal tumors may reflect a gene region interaction, where the variant does not directly determine tumor location, but rather manifests within an existing biological niche predisposed to oligodendroglial tumor formation or progression. These observations support the hypothesis that the left frontal lobe represents a relatively permissive neurodevelopmental and epigenetic environment, within which regulatory variants like rs3026809 may have maximal functional impact aligning with the spatial pattern in our cohort.

Our study focused on the potential regulatory single-nucleotide variant (G>A), which was observed in heterozygous and homozygous states among our patients. This variant has a relatively high allele frequency in global human populations; however, once the comparative genomic databases are checked, alignment of rs3026809 in 92 eutherian mammals indicated that the position where the G>A variation occurs is highly conserved. This high conservation is observed in many other species, including primates, rodents, and birds, although some species exhibit alternative bases. The strong conservation of this nucleotide suggests that it is likely critical for functional or structural purposes. Its strict preservation in primates further indicates that the rs3026809 variant may have notable functional consequences.

Further supporting this interpretation, rs3026809 is localized at predicted TF binding sites, where any single-nucleotide alteration could potentially alter the dynamics of transcription. Such regulatory region variants at this locus are of special concern since the gene has been discussed recently in the literature on glial tumorigenesis such as glial tumor differentiation, stress responses, and tumor microenvironment (98, 99). Particularly in glial tumor biology, human-specific regulatory elements are important given that fine-tuned transcriptional regulation underlies glial development, plasticity, and extended lifespan (100). As a result, in

gliomas, this regulatory baseline might influence disease progression or aggressiveness rather than tumor initiation.

Within our dataset, rs3026809 (G>A) was identified in 7/15 oligodendroglioma and 9/9 GBM patients, and critically, it was present in both tumor tissue and matched peripheral blood samples, demonstrating that this variant might not be somatic and should not be characterized as tumor specific. Still, the recurrence of this variant in a particular proportion of our cohort increases the possibility that rs3026809-A may contribute to inter-individual differences and progression kinetics in tumor biology. Although causality cannot be claimed, evolutionary conservation of this nucleotide, its proximity to regulatory elements and implication in glial neoplasia as promoted by recent literature, support the interpretation that rs3026809-A may function as a regulatory modifier with potential relevance to the transition from lower-grade (grade II) to higher-grade (grade III) oligodendroglioma and then GBMs. Not only does *ECE1* itself appear relevant, but PPI network analysis also revealed functional interactions with eight other genes, suggesting a broader role in their regulatory network. The presence of these genes in our targeted sequencing cohort was assessed, and all genes except *EDN2* were identified. Despite applying a rigorous filtering strategy, only *SLC9A1* was found to be within the targeted region. However, the *SLC9A1* variant was identified in intron 3, suggesting that it may also be considered outside the core target region of our study. Nevertheless, these findings emphasize the importance of evaluating such functionally connected genes in future studies to capture additional regulatory variants that may contribute to glioma biology.

Our analysis indicates that the *ECE1* rs3026809 (G>A) is strongly associated with glioma grade ($p=0.0082$). Pairwise comparisons revealed statistically significant enrichment in GBM relative to Oligo3 ($p = 0.005$) and all oligodendrogliomas ($p = 0.009$). Also, the variant shows a predominantly germline distribution, as supported by Hardy-Weinberg Equilibrium ($p = 0.8887$) and high blood-tumor concordance (84.2%). Although two cases displayed discordant genotypes (blood vs tumor), rs3026809 may confer a selective growth advantage in the tumor. Given that the Ki-67 index is widely used in pathology to assess tumor grade, integrating it with clinical data, *ECE1* rs3026809 as a biomarker further enhances the accuracy of tumor

characterization, as represented in our logistic regression analysis. These findings suggest that rs3026809 might contribute to malignant progression or may serve as a molecular marker for aggressive glioma.

Even 1p/19q codeletion is absent in GBM, point mutations and potential regulatory variations such as rs3026809, may arise independently of large-scale chromosomal arm losses. This region frequently harbors cis-regulatory elements, and single-nucleotide changes within these regions may alter transcription factor binding affinity or chromatin accessibility (101).

While rs3026809 and its potential regulatory association with gliomas have not been previously reported, investigating this intronic regulatory variant provides a new perspective on glioma biology. A high frequency is consistent with variants that subtly modulate tumor behavior rather than directly causing disease progression. Hence, rather than behaving as a driver variant, rs3026809 may be classified as a modifier that influences malignant tumor behavior.

Our findings should be interpreted within the context of methodological limitations. First of all, the relatively small sample size limits the strength of statistical analyses and the ability to identify definitive conclusions. Moreover, annotation using Ensembl VEP was done through variants determined in all oligodendroglioma patients, but not all downstream analyses were further performed, especially for the rare variants. For future perspective, deeper variant analysis by adding additional filtrations could enlighten the study more. *LENG9* (rs10406453), associated with prostate cancer, and *KIR2DL3* (rs62124153), linked to leukemia, are involved in DNA repair and immune regulation, respectively (102, 103). Although not yet directly associated with gliomas, their roles in key oncogenic pathways suggest potential relevance in glioma biology. Furthermore, functional validation of the identified variant was beyond the scope of this study, though it could be explored in future research. In this study only genotyping analysis was performed to correlate rs3026809 with clinical data. Further functional studies, particularly assays assessing TF binding and enhancer activity, cellular-functional or miRNA interaction assays could be pursued in future. Moreover, significant upregulation of *ECE1* in GBM supported by

differential expression analysis, suggests that expression-based approaches such as immunohistochemistry or other pathological assessments could help elucidate the clinical significance of these findings.

Additionally, due to the lack of clinical information regarding the survival outcomes of our cohort, it was not possible to perform survival analyses or carry out other prognostic assessments that could have provided further insight on rs3026809. Furthermore, since the availability of mitochondrial variation data and tumor recurrence time information were limited in our patients, statistical analyses could not be comprehensively performed. Preliminary analysis via Mann–Whitney U test showed a borderline statistically significant difference between recurrence time and *ECE1* mutation status (n=12; $p = 0.055$). Patients with *ECE1* variant showed a shorter mean recurrence time (3.56 vs. 9.67 years), suggesting a possible link to earlier recurrence. The potential clinical significance of rs3026809 in larger patient cohorts with complete clinical datasets may be further evaluated.

In addition, since all patients harbored *TERT* C228T or C250T mutations, the rs3026809 status in *TERT* wild-type glioma cases remains unknown and should be investigated in future studies. For instance, using in silico datasets such as TCGA, the presence of *ECE1* alterations could be explored across different molecular subgroups of glioma.

# 6 CONCLUSION

In this study, potential regulatory variant *ECE1* rs3026809 (G>A) was identified and characterized in oligodendrogliomas and GBMs, highlighting its potential role in glioma progression. The targeted sequencing data was confirmed using Sanger sequencing, and the variant was further screened across glioma samples using AS-PCR and RFLP. Our findings demonstrate that this variant, present in both tumor and blood samples, is predominantly a germline variant and acts as a potential regulatory modifier rather than a classic driver mutation.

Statistical analyses highlighted the relevance of rs3026809, showing a significant association with tumor grade (p=0.0082), which may influence the biological impact. Pairwise analysis showed significant associations of Oligo3 (p= 0.005) and all oligodendroglioma grades (p= 0.009) with GBM. Although no significant correlation with Ki67 index was observed, logistic regression analysis revealed strong associations with Ki67 index and tumor grade (accuracy = 90.5%). Differential expression analysis showed that *ECE1* was upregulated in GBMs compared to LGGs, supporting the role in tumor aggressiveness. Moreover, PPI network analysis revealed that *ECE1* interacts with multiple genes involved in cellular homeostasis, extracellular matrix dynamics and signaling, highlighting its regulatory role in glioma biology.

Collectively, these results highlight the significance of non-coding regulatory variants in gliomas which may provide complementary insights beyond classical markers. rs3026809 emerges as a potential biomarker for malignant progression, supported by its regulatory location, evolutionary conservation, literature evidence, and significant statistical associations. Rather than acting as a primary oncogenic driver, this variant may contribute to inter-individual differences in tumor progression, particularly in the transition to high-grade malignancy. Further studies should investigate the variant using functional assays.

# 7 REFERENCES


1. Mesfin FB, Karsonovich T, Al-Dhahir MA. Gliomas [Internet]. In: StatPearls. Treasure Island (FL): StatPearls Publishing; 2024 [updated 2024 Aug 12]. Available from: https://www.ncbi.nlm.nih.gov/books/NBK441874/
2. Lapointe S, Perry A, Butowski NA. Primary brain tumours in adults. Lancet. 2018;392(10145):432-446.
3. Ostrom QT, Gittleman H, Farah P, Ondracek A, Chen Y, Wolinsky Y, et al. CBTRUS statistical report: primary brain and central nervous system tumors diagnosed in the United States in 2007–2011. Neuro-oncology. 2014;16(Suppl 4):iv1–iv63.
4. Ghotme KA, Barreto GE, Echeverria V, Gonzalez J, Bustos RH. Gliomas: new perspectives in diagnosis, treatment and prognosis. Curr Top Med Chem. 2017;17(12):1438–1447.
5. Salam JF. Role of ATRX in DNA damage repair and PARP inhibitor sensitivity in paediatric glioblastoma [dissertation]. 2018.
6. Manjunath M, Ravichandran S, Negi H, Mitchell DC, Bhatt DL, Bhatt D, et al. Functional analysis of low-grade glioma genetic variants predicts key target genes and transcription factors. Neuro-oncology. 2021;23(4):638–649.
7. International Agency for Research on Cancer (IARC). Global Cancer Observatory [Internet]. Lyon: IARC/WHO; [cited 2024]. Available from: https://gco.iarc.who.int/en
8. American Cancer Society. Cancer Facts & Figures 2024 [Internet]. Atlanta: American Cancer Society; 2024 [cited 2024]. Available from: https://www.cancer.org/research/cancer-facts-statistics/all-cancer-facts-figures/2024-cancer-facts-figures.html
9. Shin WS, Xie F, Chen B, Yu P, Yu J, To KF, et al. Updated epidemiology of gastric cancer in Asia: decreased incidence but still a big challenge. Cancers. 2023;15(9):2639.
10. Najafi M, Majidpoor J, Toolee H, Mortezaee K. The current knowledge concerning solid cancer and therapy. J Biochem Mol Toxicol. 2021;35:e22900.
11. Tempfer CB, Reymond MA. Sporadic cancers. In: Coleman W, Tsongalis G, editors. The Molecular Basis of Human Cancer. New York (NY): Humana Press; 2017.
12. Garreffa E, Lee R. Hereditary and familial cancer. Surgery (Oxford). 2024;42(3):177–183.
13. Foulkes WD, Smith IE, Reis-Filho JS. Triple-negative breast cancer. N Engl J Med. 2010;363(20):1938–1948.
14. Lynch HT, de la Chapelle A. Hereditary colorectal cancer. N Engl J Med. 2003;348(10):919–932.
15. Malkin D, Li FP, Strong LC, Fraumeni JF Jr, Nelson CE, Kim DH, et al. Germline mutations of the p53 tumor-suppressor gene in a familial syndrome of breast cancer, sarcomas, and other neoplasms. Science. 1990;250(4985):1233–1238.
16. Stratton MR, Campbell PJ, Futreal PA. The cancer genome. Nature. 2009;458(7239):719–724.
17. Landrigan PJ, Fuller R, Acosta NJR, Adeyi O, Arnold R, Basu NN, et al. The Lancet Commission on pollution and health. Lancet. 2018;391(10119):462–512.

18. Tan N, et al. Global, regional, and national burden of early-onset gastric cancer. Cancer Biol Med. 2024;21(8):667–678.
19. Cancer Classification [Internet]. News-Medical.net. 2009. Available from: https://www.news-medical.net/health/Cancer-Classification.aspx
20. Hanahan D. Hallmarks of cancer: new dimensions. Cancer Discov. 2022;12(1):31–46. Available from: https://aacrjournals.org/cancerdiscovery/article/12/1/31/675608
21. Maldonado KA, Alsayouri K. Physiology, brain [Internet]. In: StatPearls. Treasure Island (FL): StatPearls Publishing; 2023 [updated 2023 Mar 17]. Available from: https://www.ncbi.nlm.nih.gov/books/NBK551718/
22. Jellinger KA. The Human Nervous System: Structure and Function. 6th ed. [Review]. Eur J Neurol. 2009;16:e136.
23. Ostrom QT, Francis SS, Barnholtz-Sloan JS. Epidemiology of brain and other CNS tumors. Curr Neurol Neurosci Rep. 2021;21:68.
24. Louis DN, Perry A, Wesseling P, Brat DJ, Cree IA, Figarella-Branger D, et al. The 2021 WHO classification of tumors of the central nervous system: a summary. Neuro-oncology. 2021;23(8):1231–1251.
25. Smith HL, Wadhwani N, Horbinski C. Major features of the 2021 WHO classification of CNS tumors. Neurotherapeutics. 2022;19(6):1691–1704.
26. Johnson DR, Guerin JB, Giannini C, Morris JM, Eckel LJ, Kaufmann TJ. 2016 updates to the WHO brain tumor classification system: what the radiologist needs to know. RadioGraphics. 2017;37:2164–2180.
27. Buckner JC, Brown PD, O'Neill BP, Meyer FB, Wetmore CJ, Uhm JH. Central nervous system tumors. Mayo Clin Proc. 2007;82:1271–1286.
28. American Cancer Society. Key statistics for brain and spinal cord tumors in adults [Internet]. Atlanta: American Cancer Society; [cited 2024]. Available from: https://www.cancer.org/cancer/types/brain-spinal-cord-tumors-adults/about/key-statistics.html
29. Rahman R, Janowski M, Killick-Cole CL, Singleton WGB, Campbell E, Walczak P, et al. Childhood brain tumors: a review of strategies to translate CNS drug delivery to clinical trials. Cancers. 2023;15:857.
30. Winkler F, Venkatesh HS, Amit M, Batchelor T, Demir IE, Deneen B, et al. Cancer neuroscience: state of the field and future directions. Cell. 2023;186(8):1689–1707.
31. Julich M, Oliinyk D, Grunert M, Rossler J, Lode HN. Glioblastoma: epidemiology, genetics, and therapeutic strategies. Brain Sci. 2022;12(6):722.
32. Central Brain Tumor Registry of the United States. CBTRUS Statistical Report 2005–2006 [Internet]. Hinsdale (IL): CBTRUS; 2006 [cited 2007 Aug 21]. Available from: https://www.cbtrus.org/reports/2005-2006/2006report.pdf
33. McNamara C, Mankad K, Thust S, Dixon L, Limback C, D'Arco F, et al. 2021 WHO classification of tumours of the central nervous system: a review for the neuroradiologist. Neuroradiology. 2022;64:1–32.

34. Kleihues, Paul, et al. "The WHO classification of tumors of the nervous system." Journal of Neuropathology & Experimental Neurology 61.3 (2002): 215-225.
35. Wu F, Yin Y, Fan W, Zhai Y, Yu M, Wang D, et al. Immunological profiles of human oligodendrogliomas define two distinct molecular subtypes. eBioMedicine. 2023;87:104410.
36. Terzi N, Yilmaz I, Oz A. The applicability of Haarlem integrated diagnostic system in diffuse glial tumors and the role of PDGFRA amplification as a marker of recurrence and prognosis. Balkan Med J. 2018. doi:10.4274/balkanmedj.2018.1221.
37. Stanford Medicine. Oligodendroglioma [Internet]. Stanford (CA): Stanford Medicine Brain Tumor Center; [cited 2024]. Available from: https://med.stanford.edu/brain-tumor/conditions/glioma/oligodendroglioma.html
38. Xia Y, Yang F, Wang Y, Wang Y, Wang Y, Dai C, et al. Molecular landscape of IDH-mutant astrocytoma and oligodendroglioma grade 2 indicates tumor purity as an underlying genomic factor. Mol Med. 2022;28(1).
39. Roodakker KR, Alhuseinalkhudhur A, Al-Jaff M, Georganaki M, Zetterling M, Berntsson SG, et al. Region-by-region analysis of PET, MRI, and histology in en bloc-resected oligodendrogliomas reveals intra-tumoral heterogeneity. Eur J Nucl Med Mol Imaging. 2019;46(3):569–579.
40. Fuente M. Adult-type diffuse gliomas. Continuum Lifelong Learn Neurol. 2023;29(6):1662–1679.
41. Liu S, Liu X, Xiao Y, Chen S, Zhuang W. Prognostic factors associated with survival in patients with anaplastic oligodendroglioma. PLoS One. 2019;14(1):e0211513.
42. Bund C, Guergova-Kuras M, Cicek AE, Moussallieh FM, Dali-Youcef N, Piotto M, et al. An integrated genomic and metabolomic approach for defining survival time in adult oligodendroglioma patients. Metabolomics. 2019;15(5).
43. Richardson TE, Walker JM, Abdullah KG, McBrayer SK, Viapiano MS, Mussa ZM, et al. Chromosomal instability in adult-type diffuse gliomas. Acta Neuropathol Commun. 2022;10(1).
44. Bray F, Laversanne M, Sung H, Ferlay J, Siegel RL, Soerjomataram I, et al. Global cancer statistics 2022: GLOBOCAN estimates of incidence and mortality worldwide for 36 cancers in 185 countries. CA Cancer J Clin. 2024. doi:10.3322/caac.21834.
45. Central Brain Tumor Registry of the United States. CBTRUS Fact Sheet 2024 [Internet]. Hinsdale (IL): CBTRUS; 2024 [cited 2024 Nov 1]. Available from: https://cbtrus.org/cbtrus-fact-sheet/
46. Ostrom QT, Price M, Neff C, Cioffi G, Waite KA, Kruchko C, et al. CBTRUS statistical report: primary brain and other central nervous system tumors diagnosed in the United States in 2016–2020. Neuro-oncology. 2023;25(Suppl 4):iv1–iv99.
47. Tamimi AF, Juweid M. Epidemiology and outcome of glioblastoma. In: De Vleeschouwer S, editor. Glioblastoma [Internet]. Brisbane (AU): Codon Publications; 2017. Chapter 8. Available from: https://www.ncbi.nlm.nih.gov/books/NBK470003/
48. American Association of Neurological Surgeons. Glioblastoma multiforme [Internet]. Park Ridge (IL): AANS; 2024 [cited 2024 Apr 15]. Available from: https://www.aans.org/patients/conditions-treatments/glioblastoma-multiforme/

49. Toader C, Eva L, Costea D, Corlatescu AD, Covache-Busuioc RA, Bratu BG, et al. Low-grade gliomas: histological subtypes, molecular mechanisms, and treatment strategies. Brain Sci. 2023;13(12):1700.
50. Karsonovich T, Gasalberti DP, Rayi A. Low-grade gliomas [Internet]. In: StatPearls. Treasure Island (FL): StatPearls Publishing; 2025 [updated 2025 Dec 13]. Available from: https://www.ncbi.nlm.nih.gov/books/NBK560668/
51. Oprita A, Baloi SC, Staicu GA, Alexandru O, Tache DE, Danoiu S, et al. Updated insights on EGFR signaling pathways in glioma. Int J Mol Sci. 2021;22(2):587.
52. Ostrom QT, Cioffi G, Gittleman H, Patil N, Waite K, Kruchko C, et al. CBTRUS statistical report: primary brain and other central nervous system tumors diagnosed in the United States in 2014–2018. Neuro-oncology. 2021;23(Suppl 3):iii1–iii105.
53. Olar A, Sulman EP, Aldape KD, Goodman LD, Heathcock LE, Penas-Prado M, et al. ATRX protein loss and deregulation of PI3K/AKT pathway is frequent in pilocytic astrocytoma with anaplastic features. Clin Neuropathol. 2019;38(2):59.
54. Huang LE. Impact of CDKN2A/B homozygous deletion on the prognosis and biology of IDH-mutant glioma. Biomedicines. 2022;10(2):246.
55. Oldrini B, Vaquero-Siguero N, Mu Q, Kroon P, Zhang Y, Galan-Garga M, et al. MGMT genomic rearrangements contribute to chemotherapy resistance in gliomas. Nat Commun. 2020;11(1):3883.
56. Bettegowda C, et al. Mutations in CIC and FUBP1 contribute to human oligodendroglioma. Science. 2011.
57. Weber-Levine C, et al. Genomic alterations in molecularly defined oligodendrogliomas. Neurosurgery. 2025;96(2):328–337.
58. Penkova A, Kuziakova O, Gulaia V, Tiasto V, Goncharov NV, Lanskikh D, et al. Comprehensive clinical assays for molecular diagnostics of gliomas: the current state and future prospects. Front Mol Biosci. 2023;10:1216102.
59. Tapia JC, Niechi I. Endothelin-converting enzyme-1 in cancer aggressiveness. Cancer Lett. 2019;452:152–157.
60. Kristianto J, Johnson MG, Zastrow RK, Radcliff AB, Blank RD. Endothelin-converting enzyme-1 (ECE1) is essential in adult normal physiology. Arterioscler Thromb Vasc Biol. 2015;35(Suppl 1):A195.
61. Hofstra RMW, Valdenaire O, Arch E, Osinga J, Kroes H, Buys CH, et al. A loss-of-function mutation in the endothelin-converting enzyme 1 (ECE-1) associated with Hirschsprung disease, cardiac defects, and autonomic dysfunction. Am J Hum Genet. 1999;64(1):304–307.
62. Whyteside AR, Turner AJ, Lambert DG. Endothelin-converting enzyme-1 (ECE-1) is post-transcriptionally regulated by alternative polyadenylation. PLoS One. 2014;9:e83260.
63. Niechi I, Erices JI, Reyes M, Uribe D, Rocha JD, Carrasco-Avino G, et al. Cancer stem cell and aggressiveness traits are promoted by stable endothelin-converting enzyme-1c in glioblastoma cells. Cells. 2023;12(3):506.

64. Wang Y, Li Y, Tian Q, Li Y, Fu G, Xu S, et al. CircNDC80 promotes glioblastoma multiforme tumorigenesis via the miR-139-5p/ECE1 pathway. J Transl Med. 2023;21(1):22.
65. Wan X, Zhang L, Jiang B. Role of endothelin B receptor in oligodendroglioma proliferation and survival: in vitro and in vivo evidence. Mol Med Rep. 2014;9(1):229–234.
66. Zhou T, Niu Y, Li Y. Advances in research on malignant tumors and targeted agents for TOP2A (Review). Mol Med Rep. 2025;31:50.
67. Gielniewski B, Wisniewska M, Szadkowska P, Klis K, Sierzputowska K, Stoczynska-Fidelus E, et al. Targeted sequencing of cancer-related genes reveals a recurrent TOP2A variant which affects DNA binding and coincides with global transcriptional changes in glioblastoma. Int J Cancer. 2023;153(5):1003–1015.
68. Wallace DC. Mitochondria and cancer. Nat Rev Cancer. 2012;12(10):685–698.
69. Seyfried TN, Mukherjee P. Targeting energy metabolism in brain cancer: review and hypothesis. Nutr Metab (Lond). 2005;2:30.
70. Sourty B, Dardaud LM, Bris C, Desquiret-Dumas V, Boisselier B, Basset L, et al. Mitochondrial DNA copy number as a prognostic marker is age-dependent in adult glioblastoma. Neurooncol Adv. 2022;4(1):vdab191.
71. Sun X, Vaghjiani V, Jayasekara WSN, Cain JE, St John JC. The degree of mitochondrial DNA methylation in tumor models of glioblastoma and osteosarcoma. Clin Epigenetics. 2018;10:157.
72. Soon BH, Abdul Murad NA, Then SM, Abu Bakar A, Fadzil F, Thanabalan J, et al. Mitochondrial DNA mutations in grade II and III glioma cell lines are associated with significant mitochondrial dysfunction and higher oxidative stress. Front Physiol. 2017;8:231.
73. Anna A, Monika G. Splicing mutations in human genetic disorders: examples, detection, and confirmation. J Appl Genet. 2018;59(3):253–268.
74. Clancy S. RNA splicing: introns, exons and spliceosome. Nature Education. 2008;1(1):31.
75. Choi S, Cho N, Kim EM, Park MK, Lee CH. The role of alternative pre-mRNA splicing in cancer progression. Cancer Cell Int. 2023;23:249.
76. Hagemann IS. Overview of technical aspects and chemistries of next-generation sequencing. In: Kulkarni S, Pfeifer J, editors. Clinical Genomics. Amsterdam: Elsevier; 2015. p. 3–19.
77. Gomes A, Korf B. Genetic testing techniques. In: Pediatric Cancer Genetics. Philadelphia (PA): Elsevier; 2018. p. 47–64.
78. Newton CR, Graham A, Heptinstall LE, Powell SJ, Summers C, Kalsheker N, et al. Analysis of any point mutation in DNA: the amplification refractory mutation system (ARMS). Nucleic Acids Res. 1989;17(7):2503–2516.
79. Gaudet M, Fara AG, Beritognolo I, Sabatti M. Allele-specific PCR in SNP genotyping. In: Komar AA, editor. Single Nucleotide Polymorphisms: Methods and Protocols. 2nd ed. Totowa (NJ): Humana Press; 2009. p. 415–424.
80. Di Felice F, Micheli G, Camilloni G. Restriction enzymes and their use in molecular biology: an overview. J Biosci. 2019;44:38.

81. Marwal A, Gaur RK. Molecular markers: tool for genetic analysis. In: Animal Biotechnology. Academic Press; 2020. p. 353–372.
82. Tomczak K, Czerwinska P, Wiznerowicz M. The Cancer Genome Atlas (TCGA): an immeasurable source of knowledge. Contemp Oncol (Pozn). 2015;19(1A):A68–77.
83. Hunt SE, McLaren W, Gil L, Thormann A, Schuilenburg H, Sheppard D, et al. Annotating and prioritizing human variants with the Ensembl Variant Effect Predictor: a tutorial. Hum Mutat. 2022;43(8):986–997.
84. Rauluseviciute I, Riudavets-Puig R, Blanc-Mathieu R, Castro-Mondragon JA, Ferenc K, Kumar V, et al. JASPAR 2024: 20th anniversary of the open-access database of transcription factor binding profiles. Nucleic Acids Res. 2024;52(D1):D174–D182.
85. Dong S, Boyle AP. Annotating and prioritizing human non-coding variants with RegulomeDB v. 2. Nat Genet. 2023;55(5):724–726.
86. GTEx Consortium. The Genotype-Tissue Expression (GTEx) pilot analysis: multitissue gene regulation in humans. Science. 2015;348(6235):648–660.
87. Vella D, Marini S, Vitali F, Di Silvestre D, Mauri G, Bellazzi R. MTGO: PPI network analysis via topological and functional module identification. Sci Rep. 2018;8(1):5499.
88. Weber F, Knapp G, Anbari F, Kuss O, Glass A. Zero-cell corrections in random-effects meta-analyses. Res Synth Methods. 2020;11(6):913–919.
89. Mansouri A, Karamchandani J, Das S. Molecular genetics of secondary glioblastoma. In: De Vleeschouwer S, editor. Glioblastoma [Internet]. Brisbane (AU): Codon Publications; 2017. Chapter 2. Available from: https://www.ncbi.nlm.nih.gov/books/NBK469981/
90. Tseng CC, Chen YJ, Chang WC, Lan TH, Chen CH, Shih WL, et al. Genetic variants in transcription factor binding sites in humans: triggered by natural selection and triggers of diseases. Int J Mol Sci. 2021;22(8):4187.
91. Nielsen LAG, Brems H, Callaerts-Vegh Z, D'Hooge R, Bhatt DL, Bhatt D, et al. Evaluation of the proliferation marker Ki-67 in gliomas: interobserver variability and digital quantification. Diagn Pathol. 2018;13(1):38.
92. Sun L, Li K, Gao F. Difference of expression of tumor-related markers in gliomas tissues between Uygur and Han nationalities patients with gliomas in Xinjiang. Chin J Clin Neurosurg. 2019;24:75–77.
93. Kusaczuk M, Kretowski R, Bartoszewicz M, Cechowska-Pasko M. Cellular stress responses as modulators of drug cytotoxicity in pharmacotherapy of glioblastoma. Biochim Biophys Acta Rev Cancer. 2024;1879(1):189054.
94. Kuruppu S, Smith AI. Endothelin converting enzyme-1 phosphorylation and trafficking. FEBS Lett. 2012;586(16):2212–2217.
95. Zhou W, Ruan H, Zhu L, Chen S, Yang M. Unveiling a novel glioblastoma deep molecular profiling: insight into the cancer cell differentiation-related mechanisms. ACS Omega. 2025.

96. Kamoun A, de Reynies A, Idbaih A, Criniere E, Marie Y, Dehais C, et al. Integrated multi-omics analysis of oligodendroglial tumours identifies three subgroups of 1p/19q co-deleted gliomas. Nat Commun. 2016;7(1):11263.
97. Poncet S, Renard E, Boulanger C, Devos P, Bendriss-Vermare N, Bendriss-Vermare N, et al. The expression and function of the endothelin system in contractile properties of vaginal myofibroblasts of women with uterovaginal prolapse. Am J Obstet Gynecol. 2005;192(2):426–432.
98. Yang J, Li Z, Zhang Q, Liang G, Yan M, Lin Y, et al. Circular RNA PTPN4 contributes to blood-brain barrier disruption during early epileptogenesis. Adv Sci. 2025;e02250.
99. Park G, Jin Z, Lu H, Du J. Clearing amyloid-beta by astrocytes: the role of Rho GTPases signaling pathways as potential therapeutic targets. Brain Sci. 2024;14(12):1239.
100. Won H, de la Torre-Ubieta L, Stein JL, Parikshak NN, Huang J, Opland CK, et al. Human evolved regulatory elements modulate genes involved in cortical expansion and neurodevelopmental disease susceptibility. Nat Commun. 2019;10(1):2396.
101. Decaesteker B, Durinck K, Van Roy N, De Wilde B, Van Neste C, Van Haver S, et al. From DNA copy number gains and tumor dependencies to novel therapeutic targets for high-risk neuroblastoma. J Pers Med. 2021;11(12):1286.
102. Gao L, et al. Development and validation of a six-RNA binding proteins prognostic signature and candidate drugs for prostate cancer. Genomics. 2020;112(6):4980–4992.
103. Liu W, et al. The KIR2DL family serves as prognostic biomarkers and correlates with immune infiltrates in acute myeloid leukaemia. J Cell Mol Med. 2024;28(8):e18256. doi:10.1111/jcmm.18256

# 8 APPENDIX

## 8.1 Patient Informed Consent Form

## 8.2 Ethics Committee Approval

## 8.2 Ethics Committee Approval (Continue)

## 8.3 MOKAD Congress

## 8.4 MOKAD Congress (Continue)

# 9 CURRICULUM VITAE